Mechanical and fire tests on thermal breaks attached to concrete supports

A. Ben Larbi, M. Couchaux, C. Thauvoye, C. Sautot

Mechanical and fire tests on thermal breaks attached to concrete supports

A. BEN LARBI[a], M. COUCHAUX[b], C. THAUVOYE[a], C. SAUTOT[c]

[a] *Centre Technique Industriel de la Construction Métallique, Espace technologique L'orme des merisiers, Immeuble Apollo, 91193 Saint-Aubin, France*

[b] *Institut National des Sciences Appliquées de Rennes, 20 Avenue des Buttes de Coësmes, 35708, Rennes, France*

[c] *Institut Supérieure des Matériaux et Mécaniques Avancées, 4 Avenue Frédéric Auguste Bartholdi, 72000, Le Mans, France*

ABSTRACT

This paper deals with the mechanical and fire behaviour of simple solutions of thermal breaks for external steel structures (balconies, passageways, solar panels …) attached on a concrete facade with external thermal insulation. The proposed solutions are composed of a PVC or plywood layer implemented between an extended end-plate connection and the concrete support (lintel, floor slab, concrete wall). A total of 12 monotonic mechanical tests have been performed on steel-to-concrete connections using intermediate insulation layers (PVC or plywood) in order to investigate the rotational stiffness, plastic/ultimate bending moments, the rotation capacity as well as the failure mode. Two types of fastening were used; bolted embedded end-plates and post-installed mechanical/chemical fasteners. In order to evaluate the influence of the studied solutions of thermal breaks on the behaviour of a balcony under fire, two external flame experimental tests were carried out on realistic balconies attached to a concrete support. These fire tests demonstrated that the implementation of the proposed thermal breaks between end-plates and the support does not affect the stability of the balconies subjected to fire.

Keywords: *Buildings; attached steel structure; thermal breaks; concrete support; mechanical tests; fire tests.*

1. Introduction

For the building industry, one of the biggest challenges right now is to reduce the impact of buildings on the environment by reducing overall energy demand and CO_2 emissions. The construction of Nearly Zero-Energy Buildings (NZEB) becomes a vital necessity [1]. NZEB requires the improvement of the energy efficiency of buildings, and thus reducing heat losses from envelope. Although improving thermal performances of the envelope components seems to be easy to reach, the problem of singular points and interfaces between materials need to be solved. In most cases, the singular points need to be analysed considering the interaction between various normative requirements. The case of thermal breaks that must meet thermal, mechanical and often fire performances requirements is a good illustration.

Thermal breaks are systems used to reduce heat loss through thermal bridges. Linear or point thermal bridges are parts of the building envelope, where the otherwise uniform thermal resistance varies significantly. Point thermal bridges typically occur where an insulated wall is perforated (penetration) by an element with high thermal conductivity. They are characterised by a point thermal transmittance (χ-value in W/K). It is possible to reliably determine the heat transfer through a thermal bridge via numerical methods using finite element or finite difference methods [2] in accordance with methods specified in EN ISO 10211 [3]. The implementation of external steel structures, such as balconies, on a facade with external thermal insulation, reduces thermal bridges, compared to concrete structures, due to the point fixings on the support instead of continuous extension of the floor slab [4]. However, the thermal performance can be further improved using thermal breaks between the external steel structure and the support. Thermal breaks can be either standard manufactured products proposed by industrial suppliers or simpler solutions implemented by companies. The advantages of these solutions are their reduced costs and ease of erection. A simple solution consists in inserting an intermediate layer between the end-plate of the steel beam and the steel/concrete support. This kind of solution has attracted a lot of attention during the recent years by varying the insulating material. Nasdala et al [5] and Sulcova et al [6] performed numerical simulations and adapted the Eurocode 3 component

approach to take into account the intermediate layer. The thickness of the layer as well as the friction coefficients influence strongly the final behaviour of the connection. Cleary et al [7] loaded under bending and shear force thermal break composed of Fiber Reinforced Resin and highlighted a decrease of the stiffness of the connection. Peterman et al ([8], [9]) demonstrated that Fiber-Reinforce Polymer don't modify significantly the behaviour of the connection and don't yield in compression. Hamel and White [10] used neoprene as intermediate layers and obtained low rotational stiffness and bending resistance mainly as a result of a significant crushing of neoprene in the compressive area caused by the bending moment. Ben Larbi et al [11] drawn similar conclusions inserting elastomer in conjunction with PVC. However, the decrease of the ultimate bending resistance was quite limited. Elastomer and neoprene are too flexibles for moment resisting connections. More rigid solutions such as PVC or wood seems to be necessary to guarantee a minimum rigidity of the connection and to limit the deflections of the balconies. Moreover, this solution is clearly cheaper than Fiber Reinforced Polymer.

Solutions of thermal breaks composed of a PVC or plywood intermediate layers placed between end plates of beam attached to a steel or concrete support have been studied in the framework of the French ADEME (Environment and energy management Agency) project TREPOS [12]. The first results of this project concern the thermal and mechanical performances for external steel structures attached on a steel support [13]. These solutions were able to reduce the thermal bridge by 40 to 50 % and achieve around 70% of the performances of industrial solutions [12]. The various mechanical test campaigns have shown that thermal breaks with extended end-plate can develop an interesting behaviour with regard to the mechanical strength requirements of steel cantilever beam and in particular the deflection criteria. Thermal breaks composed of stiffened extended end-plate can develop a behaviour similar to that of a conventional non-stiffened end-plate. These results for thermal break connecting steel beam to steel support were encouraging. However, in practice many steel balconies are also connected to concrete support. Investigations are thus needed to estimate the behaviour of these solutions of thermal breaks in this situation. Ben Larbi et al [11] characterized solutions of thermal breaks

attached to concrete block with passing through anchor bolts, but this anchoring system was different from common practices. In addition, the intermediate insulating layers, composed of elastomer (for acoustic insulation) and PVC, were clearly more flexible. It is thus necessary to analyse more realistic anchoring system such as post-installed fasteners or bolted embedded plates with intermediate insulating layer made of PVC or plywood that develop an interesting mechanical response for the connection of external steel structure to a steel support [13]. The numerical study performed in the framework of TREPOS project [12] highlighted that the proposed solution attached to concrete support reduces the thermal bridge (χ) by about 35 to 50% in comparison with a connection without thermal break, and are able to achieve around 70% of the thermal performances of industrial solutions but are 5 to 10 times less expensive.

The fire resistance is generally required for the attached steel structure in façade. In this case, it should ensure the good structural performance of the attached structure with thermal breaks. The use of specific materials for thermal breaks, such as PVC, FRP/FRR or plywood, could lead to a loss of mechanical strength at high temperatures when these items are subjected to the flames coming out of the façade openings. Moreover, the attached steel structure may have a significant role to reduce the risk of fire spread to upper levels [14]. Therefore, it is essential that the sealing hot gases and flames is ensured at the junction between the attached structure and the facade. Among European countries, several tests exist to assess the impact of flames on a façade. They are oriented toward fire reaction and the LEPIR II, a French large-scale test, is one of them. It can be used as a basis to test the fire resistance of a structure. Within the framework of the project TREPOS, the LEPIR II test setup was adapted and used for that goal to test balconies with and without thermal breaks.

The present paper gives the results of a study assessing the mechanical and fire behaviour of simple solutions of thermal breaks composed of a PVC or plywood layer implemented between extended end-plate connections of steel beams and concrete support (lintel, floor slab, concrete wall). Monotonic tests performed on 12 cantilever beams attached with and without the proposed solution of thermal break are presented in section 2. The connections were subjected

to major bending moment and minor shear force typically applied to connections of balconies. Two types of mechanical fastening typically used in practice have been studied; post-installed mechanical/chemical fasteners and bolted embedded plates. The effect of bolt arrangement and properties of thermal insulating layers were also studied and particularly the impact on the rotational stiffness, plastic/ultimate bending resistance and failure mode. The results of two fire tests performed on balcony attached with and without thermal breaks are presented in section 3. During these fire tests, the LEPIR II test setup was adapted. These tests highlight the effect of the presence of external thermal insulation around the connection of the balcony as well as the impact of the intermediate insulating layer on the global behaviour of the balcony.

2. Mechanical tests

2.1. Introduction

The proposed solution of thermal break has been characterized mechanically by monotonic tests on connections attached to concrete structures composed of a lintel and a slab. The objective was to study the impact of the type of material constituting the intermediate insulating layer (PVC, plywood), the shape of the steel beam (IPE, RHS or SHS) and the type of anchoring system: post-installed chemical/mechanical fasteners or bolted embedded plates. This later parameter is crucial as it affects the resistance of the tensile area and thus the bending moment resistance of the connection. In previous experimental campaign on thermal breaks attached to a concrete block [11], failure was governed by anchor bolt rupture in tension. The present campaign was designed to obtain realistic failure modes and observe possibly failure of the concrete components such as concrete cone/edge failure.

2.2. Test presentation

2.2.1. Test set-up

The test set-up presented in Figure 1 is representative of a balcony attached to a concrete slab and a lintel. A load-jack apply a vertical force at 1150 mm from the connection in order to

produce the bending moment due to gravity loading that are significant for the connection of a cantilever balcony. The concrete block is maintained at the front and the back by two rectangular steel frames. On the front side, the concrete block is placed directly on two neoprene supports resting on the lower beam of steel frame A. At the back (portal frame B), rollers are welded to a load distribution plate positioned on the concrete block (see Figure 1). Lateral supports located at mid-length of the beam were used to prevent lateral torsional buckling of the steel profile.

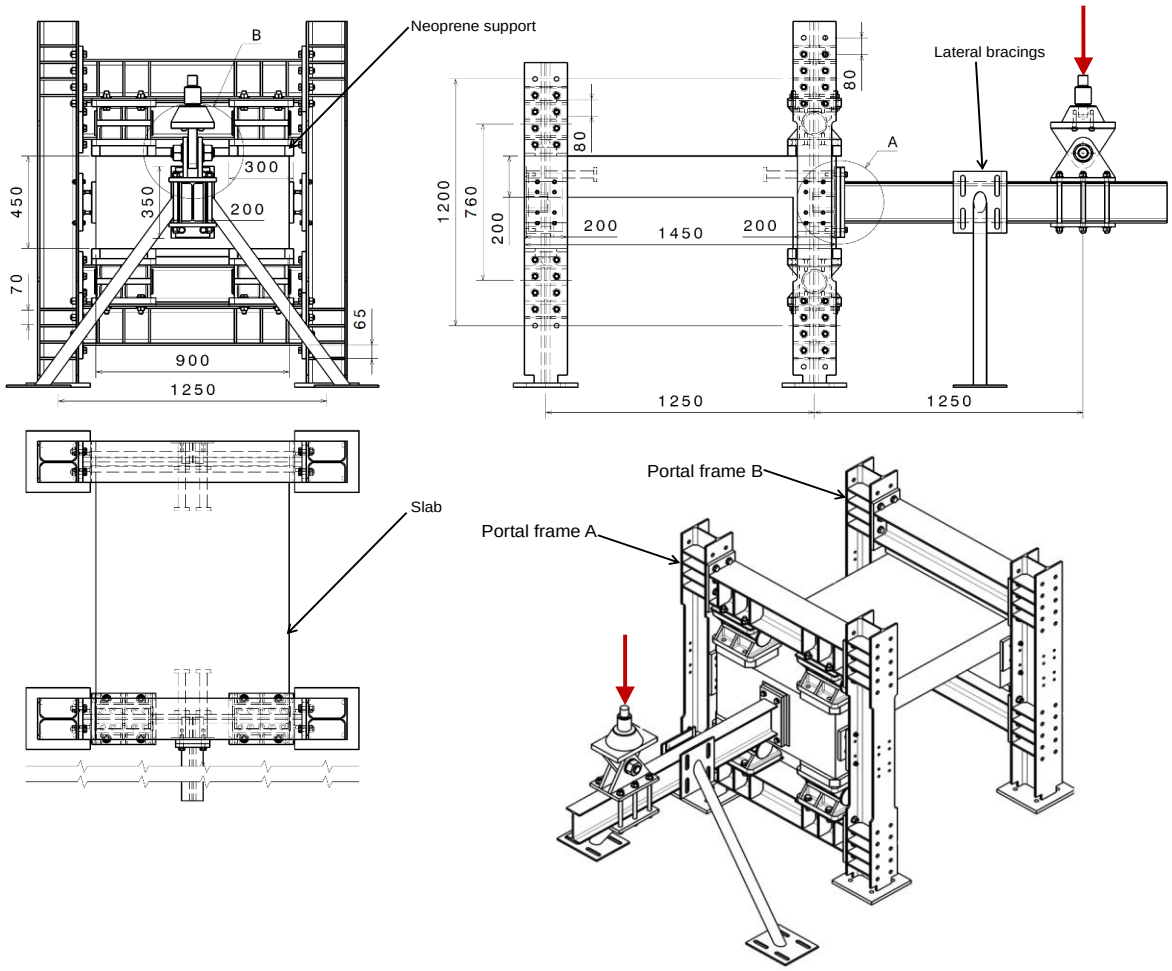

Figure 1 : *Mechanical test set-up (dimensions in mm)*

2.2.2. Connection geometry

The connection geometries have been defined in order to test the influence of the materials used as thermal insulation (PVC or plywood), the configuration of the connection (stiffened or non-stiffened extended end-plate), the shape of the beam attached (I-beam section,

rectangular/square tubes) and the anchoring system (chemical/mechanical post-installed fasteners, bolted embedded plates). The end-plates are made of S235 steel. The bolts are M16 class 8.8. The IPE 200s are made of S275 steel and the tubes of S355. For connections RTPB-1-P/B, RTPB-2-P/B and RTPB-3-P, the thickness of PVC and plywood are equal to 20 mm and 30 mm, respectively. Connection RTPB-5-P1 use PVC of 10 mm thickness. The main geometric parameters used are shown in Figure 2 and Table 1. The bolt length is equal to 60 mm for end-plate directly bolted to embedded plates (PB-1, PB-2 and PB-3) but to 90 mm in presence of intermediate later. Bolts are fully and partially threaded respectively for the length of 60 and 90 mm.

Table 1. *Geometry of specimens tested*

Specimen	Beam	t_p	t_a	Insulating	Anchoring	Stiffener	Concrete block
PB-1	IPE200	20	-	-	Embedded plate n°2	No	B3-1
RTPB-1-P	IPE200	20	20	PVC	Embedded plate n°2	No	B2-1
RTPB-1-B	IPE200	20	30	Plywood	Embedded plate n°2	No	B3-1
PB-2	IPE200	15	-	-	Embedded plate n°1	Yes	B1-1
RTPB-2-P	IPE200	15	20	PVC	Embedded plate n°1	Yes	B1-1
RTPB-2-B	IPE200	15	30	Plywood	Embedded plate n°2	Yes	B2-2
PB-3	RHS 200×120×6	20	-	-	Embedded plate n°2	Yes	B3-2
RTPB-3-P	RHS 200×120×6	20	20	PVC	Embedded plate n°2	Yes	B3-3
PB-4	IPE200	15	-	-	Post-inst. HIT-Z-R	Yes	B1-2
RTPB-4-P	IPE200	15	20	PVC	Post-inst. HIT-Z-R	Yes	B1-2
PB-5	SHS 80×5	10	-	-	Post-inst. HST 3	No	B3-3
RTPB-5-P1	SHS 80×5	10	10	PVC	Post-inst. HST 3	No	B3-2

Embedded plates have been designed to carry the bending resistance of the connection and are composed of four rods threaded to be bolted. A shear lug permit to transmit the shear force. A washer plate of 60×135×10 is welded to the lower and upper rods for Embedded plate n°1 (see Figure 2-b). For embedded plate n°2, a washer plate of 60×60×10 was welded on each upper rod (see Figure 2-a/c). The dimensions of these embedded plates were reduced to ease its implementation in steel reinforcements of the lintel.

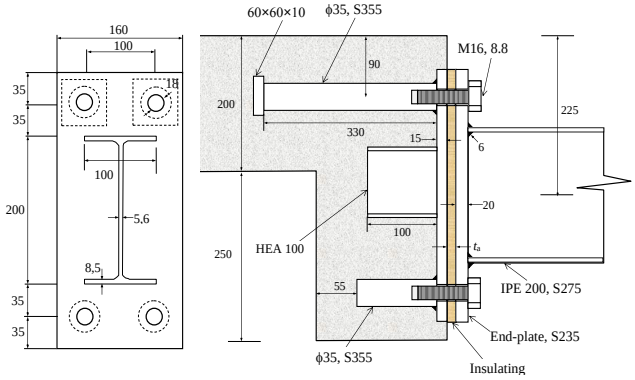

a) PB-1, RTPB-1-P/B

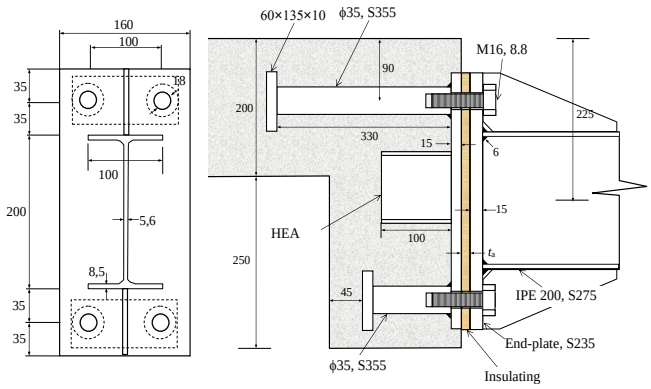

b) PB-2, RTPB-2-P/B

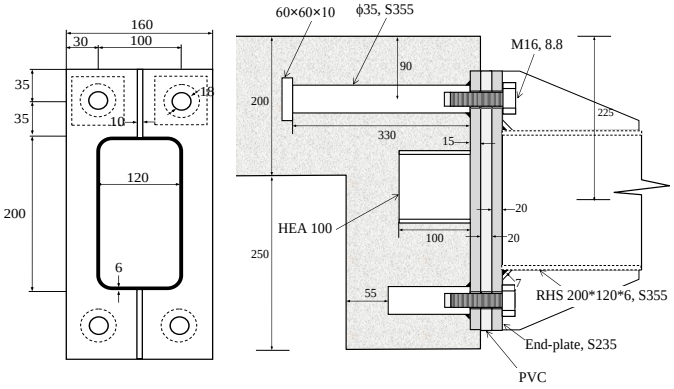

c) PB-3, RTPB-3-P

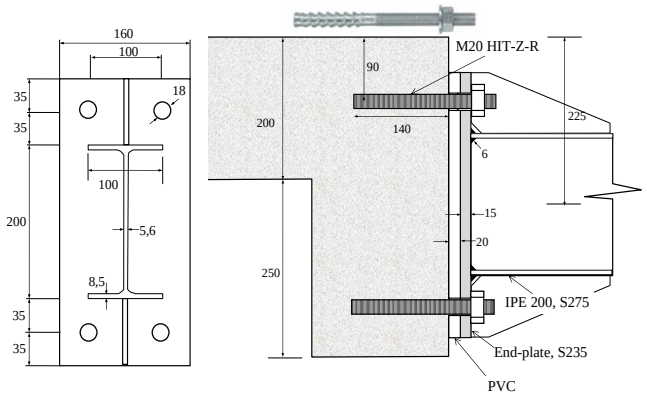

d) PB-4, RTPB-4-P

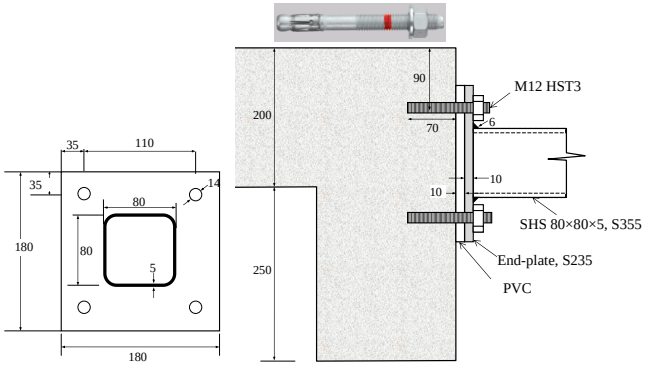

e) PB-5, RTPB-5-P1

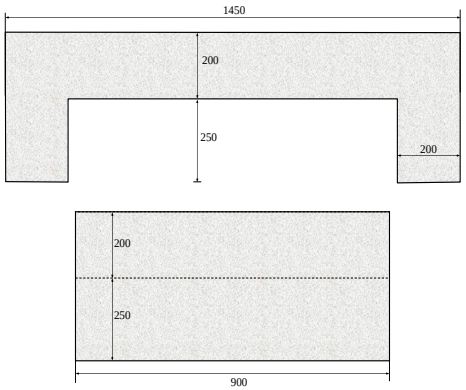

f) Concrete block (lateral and front view)

Figure 2. *Geometry of specimens tested (dimensions in mm)*

Connections PB-1 and RTPB-1-P/B (see Figure 2-a) correspond to unstiffened extended end-plate with I-beam and end-plate of 20 mm and are similar to connections PA-1 and RTPA-1 attached to steel support [13]. However, the end-plate thickness has been increased to limit prying effect and weld tearing in the tensile area. The end-plate is bolted to an embedded plate with shear lug and four rods.

Connections PB-2 and RTPB-2-P/B (see Figure 2-b) are made of stiffened extended end-plate of 15 mm thickness and are similar to connection RTPA-5-P attached to a steel support [13]. For thermal breaks attached to steel structures, it was highlighted that stiffeners increase significantly the mechanical properties under monotonic and cyclic loadings. The end-plate is also bolted to an embedded plate with shear lug and four rods.

Specimens PB-3 and RTPB-3-P (see Figure 2-c) are composed of stiffened extended end-plate connecting a RHS 200×120×6. These connections are similar to specimens PA-4 and RTPA-4-P attached to steel support [13] but the end-plate thickness is increased to 20 mm in order to limit weld tearing at failure. The end-plate is also bolted to an embedded plate with shear lug and four threaded rods.

The steel connection of PB-4 and RTPB-4-P (see Figure 2-d) is similar to that of PB-2 and RTPB-2-P but it is connected to the concrete block by means of post-installed chemical fasteners HIT-Z-R M20 with an embedded length of 140 mm. This solution can be used in the case of rehabilitation of concrete building.

The steel connection of PB-5 and RTPB-5-P1 (see Figure 2-e) is identical to that of PA-6 and RTPA-6-P1 [13] and is fastened by post-installed mechanical fasteners HST3 with an embedded length of 70 mm.

The dimensions of the concrete block, presented in Figure 2-f, are typically used in practice with a slab and a lintel of 20 cm thickness. The height of the lintel, equal to 45 cm and widely used in practice, has been chosen to maximise the lever arm of the connection and thus mechanical properties. The concrete block were casted in three times (B1, B2 and B3) and one block was used for two tests except B2-1 and B2-2 that failed during the first test by rupture of the slab reinforcements. Hence reinforcement of concrete block B2 were typical of common practice. The steel reinforcement consists in a steel reinforcing mesh ST 25C. The cover to reinforcement was 25 mm. Additional C-shape plain round bars were placed along the support zones. Shear reinforcements were added near the supports. For blocks B1 and B3, HA 12 of steel grade S500 were added to avoid concrete slab failure due to bending and permit to reach

the full capacity of the connection. The reinforcement of concrete blocks B1 and B3 is presented in Appendix A. Concrete block B2 is identical to block B3 except that the HA 12 have not been added.

2.2.3. Loading-procedure

Specimens were subjected to a monotonically increasing vertical force. All specimens were tested under displacement controlled loading. The loading was divided into elastic and plastic phases. The load range applied to the specimen during the first phase was estimated by ensuring that the connection remains elastic. The elastic phase consisted in three equal amplitude loading-unloading cycles with the load magnitude being equal to 50% of the elastic loading F_{el} and a fourth cycle where the load is increased to the full elastic loading. This loading was equal to 20 kN for all specimens except for PB-5 and RTPB-5-P1 where it was limited to 2,5 kN. In the final phase, specimens worked in the plastic domain and were loaded until failure of one or more connection components.

2.2.4. Instrumentation

Displacement transducers (LVDT) were positioned to measure the displacements at different locations of the test specimen as shown in Figure 3. Displacement sensors (V_1 to V_8 and U_1 to U_4) allowed a complementary estimation of the rotation. Finally, four displacement sensors placed horizontally were used to evaluate the crushing of the thermal insulation (U_{b1} and U_{b2}), and the elongation of the tensile part of the connection (U_{t1} and U_{t2}). An inclinometer, I_2, was positioned on the beam web at half the beam height from the connection and another one on the concrete slab, I_1.

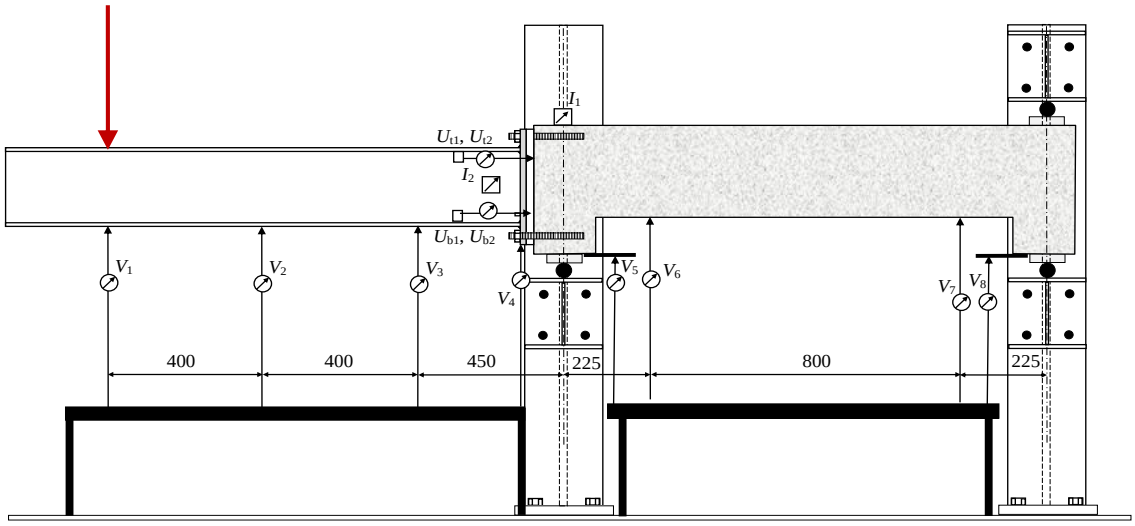

Figure 3 *– Displacement transducers and inclinometers (dimensions in mm)*

2.3. Mechanical characterization

Steel coupons were extracted from the IPE 200 beams, end-plates and bolts (3 coupons per samples) whose average mechanical characteristics are listed in Table 2. An extensometer was used at the mid-gage of the samples to estimate the Young modulus.

Table 2. *Mechanical properties of steel components*

Component	Young Modulus	Yield strength	Ultimate strength	Necking
	N/mm^2	N/mm^2	N/mm^2	%
End-plate 15 mm	206355	277,5	446,8	70
End-plate 20 mm	206140	229,1	396,7	63
IPE 200 web	220255	340,1	483,5	64
IPE 200 flange	218827	333,0	489,9	65
Bolt M16 8.8 L90	198004	1063,5	1082,2	69
Bolt M16 8.8 L60	210000(1)	1022	1056	69
Anchor bolt HIT-Z-R M20	188765	724,4	764,5	78

(1) This value correspond to the nominal one's because of the absence of reliable results

PVC and plywood were from the same samples as those used for tests on thermal breaks attached to steel structures [13], the corresponding mechanical properties are presented in this reference. For each tests, 3 concrete cylinders have been tested under compression the day of the test. The average concrete compressive strengths are summarized in Table 3 for each test.

Table 3. *Average concrete compressive strengths*

Test ID	f_{cm}
-	N/mm^2
PB-1	35,3
RTPB-1-P	27,8
RTPB-1-B	34,6
PB-2	34,1
RTPB-2-P	33,6
RTPB-2-B	31
PB-3	38,0
RTPB-3-P	36,7
PB-4	36,2
RTPB-4-P	34,1
PB-5	36
RTPB-5-P1	35,7

2.4. Mechanical test results

The moment rotation curves of the different types of connections are compared in Figure 4. The rotation of the connection is evaluated with the displacement transducers U_t and U_b. In addition the following parameters are extracted and provided in Table 4:

- the **secant rotational stiffness** $S_{j,sec}$ evaluated for $2/3M_{j,pl}$,
- the **plastic bending moment** $M_{j,pl}$ calculated according to ECCS requirements [15] that corresponds to the frontier between the elastic and elasto-plastic ranges of behaviour,
- the **ultimate bending moment** $M_{j,u}$ corresponding to the maximum bending moment applied during tests,
- elements that yield/crack before failure and the **failure mode**.

Table 4. *Rotational stiffness's, failure modes, plastic/ultimate bending moments*

Connection	$S_{j.sec}$	$M_{j.pl}$	$M_{j.u}$	Failure mode	Yielding/cracking
	kNm/rad	kNm	kNm	-	-
PB-1	8452	50,4	71,6	Bolt	Bolt, end-plate, slab, lintel
RTPB-1-B	8371	33,0	80,7	Bolt	Bolt, end-plate, slab, lintel, wood
RTPB-1-P	5207	30,0	61,6	Reinforcement	Bolt, end-plate, slab, lintel, PVC
PB-2	21134	47,6	86,0	Bolt	Bolt, end-plate, slab, lintel, weld
RTPB-2-B	13043	32,6	54,9	Reinforcement	end-plate, slab, lintel, wood
RTPB-2-P	5259	37,6	91,5	Bolt	Bolt, end-plate, slab, lintel, PVC
PB-3	7518	52,7	80,8	Bolt	Bolt, slab, lintel
RTPB-3-P	6165	42,0	72,6	Bolt	Bolt, slab, lintel, PVC
PB-4	7617	41,0	46,8	Concrete edge	Concrete, end-plate
RTPB-4-P	7748	28,6	38,5	Concrete edge	Concrete, PVC
PB-5	530	3,3	6,6	Concrete cone/sliding	Concrete, end-plate
RTPB-5-P1	526	3,4	6,0	Concrete cone/sliding	Concrete, end-plate, PVC

Four types of failure modes have been obtained depending on the anchoring system. For embedded end-plates with concrete slab sufficiently reinforced (blocks B1 and B3), the failure corresponds to bolt rupture in tension with or without end-plate yielding. End-plate yielding was observed for configurations PB-1 and PB-2 and thus in presence of non-stiffened extended end-plate, and stiffened extended end-plate of 15 mm thickness. The addition of intermediate insulating layers did not affect the final failure mode. The same results can be drawn for the proposed solution of thermal break attached to a steel support [13].

On the contrary, when the concrete slab was not sufficiently reinforced (using only steel reinforcing mesh ST 25C), the final failure was caused by rupture of reinforcement of the ST 25 C mesh (see Figure 5-b). The bending resistance of the connection was greater than the capacity of the slab in bending. For post-installed chemical fasteners (connections PB-4 and RTPB-4-P), concrete edge failure is obtained and the addition of intermediate insulating layer does not affect significantly the result. For post-installed mechanical fastener (PB-5 and RTPB-5-P1), the failure corresponds to anchor bolt sliding and finally concrete cone failure.

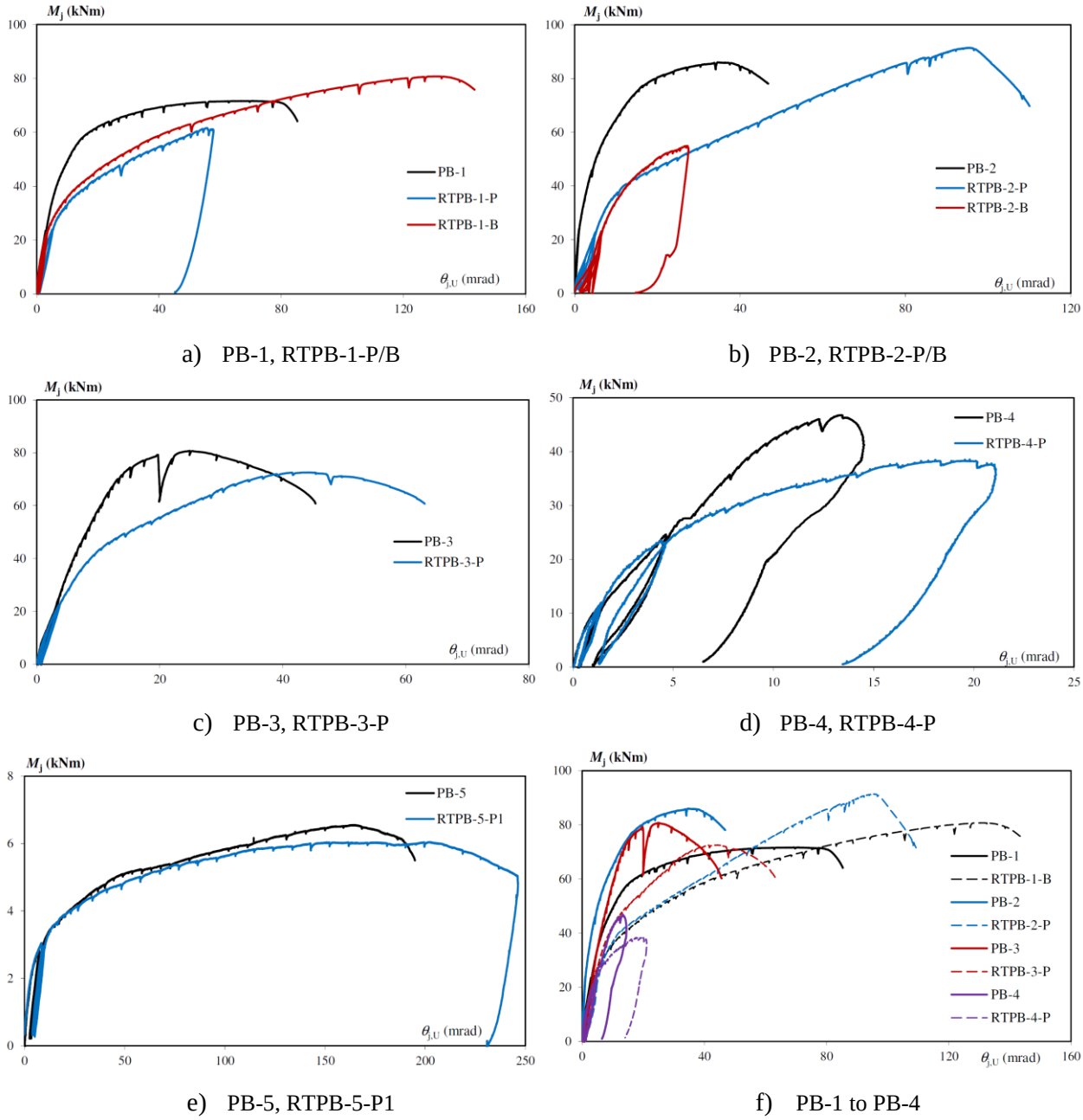

a) PB-1, RTPB-1-P/B

b) PB-2, RTPB-2-P/B

c) PB-3, RTPB-3-P

d) PB-4, RTPB-4-P

e) PB-5, RTPB-5-P1

f) PB-1 to PB-4

Figure 4. *Moment-rotation curves*

266

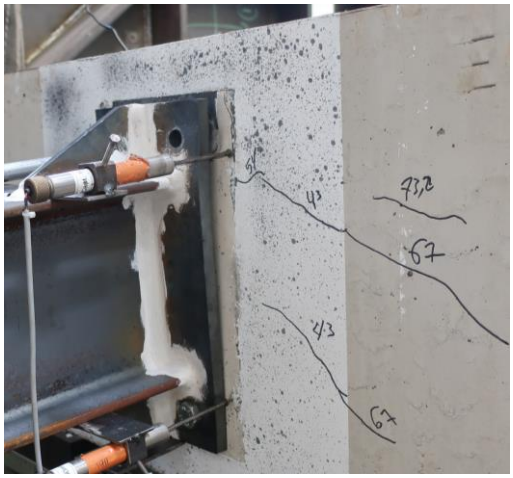

a) Lintel cracking

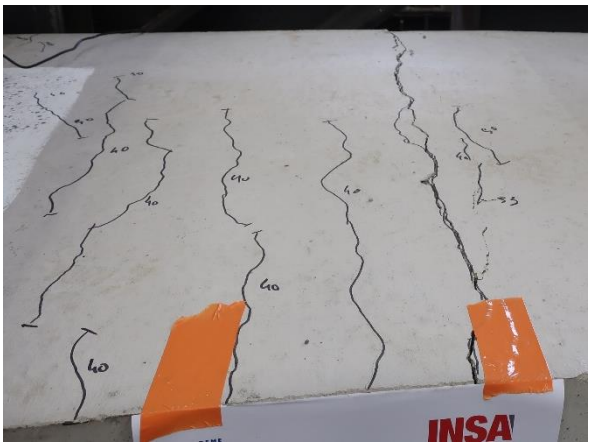

b) Slab reinforcement rupture

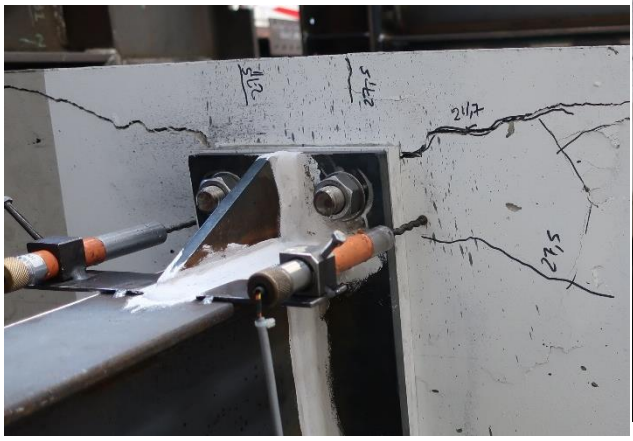

c) Concrete edge failure

d) Concrete cone failure/anchor sliding

Figure 5. *Concrete lintel and slab cracking and failure*

A yield line parallel to the beam flange develops on the end-plate in the tensile area for PB-1 and RTPB-1-P/B (see Figure 6). The deformation of RTPB-1-P is less pronounced due to an early failure of concrete slab reinforcements. End-plate yielding is the main source of ductility of connection PB-1. For connections using insulating layer, yielding in compression of the layer also affects the rotation capacity and explains its increase comparatively to the conventional connection (see Figure 4-a). The addition of plywood and PVC decreases the secant stiffness of 1 % and 38 %, respectively. This difference between the two materials is quite surprising comparatively to results obtained with other configurations but can be partially explained by different initial preloading and the variability of plywood mechanical properties. The plastic bending moment decrease of 34 % and 40 % with the addition of plywood and PVC,

277 respectively. This reduction is caused by the yielding of the insulating layer, PVC or plywood,
278 in the compressive area that appears before end-plate yielding in the tensile area. For the three
279 connections cracks, initiate on the lintel close to the upper face of the end-plate for a bending
280 moment of 45-50 kNm and propagate to the support (see Figure 5-a). A similar trend was
281 observed for connections of IPE 200 and RHS 200. Cracks also develop on the slab but with a
282 final rupture of steel reinforcements for RTPB-1-P. For PB-1, the prying force is positioned at
283 the outer edge of the end-plate (see Figure 6-a) whereas for specimens RTPB-1-P/B, the contact
284 area extends between the free edge of the end-plate and the bolts (see Figure 6-b/c). A similar
285 trend was observed for the proposed solution of thermal breaks attached to a steel support [13].
286 In presence of intermediate layer, the contact between the end-plate and the layer extends from
287 the extended end-plate to a portion of the beam web in the compressive area (see Figure 6-b/c).
288 In absence of thermal break, the compression area only develop at the bottom of the extended
289 end-plate. The use of plywood increase the ultimate bending resistance of 12,7 % (see Table 4).
290 This difference can be explained by the fact that the length of the threaded area is different for
291 specimens with and without thermal insulating layers but also by the reduction of prying effect
292 in presence of intermediate layer. The tensile resistance of bolts can be affected by the length of
293 the threaded area ([16], [17]). Hence, the connections without insulating layers used bolts that
294 were fully threaded of 60 mm length. On the contrary, the connections with thermal break used
295 partially threaded bolts of 90 length whose tensile resistance is potentially higher. The addition
296 of an intermediate layer also reduce prying effects. This difference was not observed for thermal
297 breaks attached to a steel structure [13] because the same bolts were used.

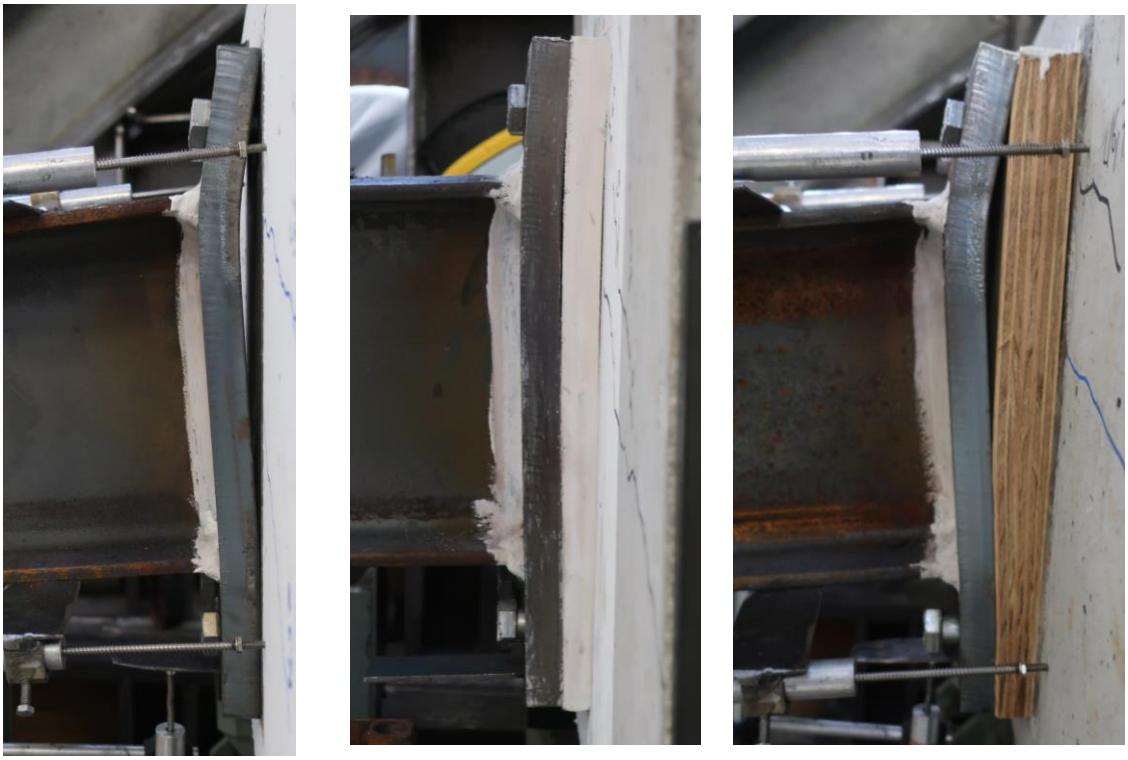

a) PB-1 b) RTPB-1-P c) RTPB-1-B

***Figure 6** – Deformed shape of specimens PB-1, RTPB-1-P/B at failure*

298 For stiffened extended end-plates with I-profile, the addition of intermediate insulating layers
299 modifies significantly the moment-rotation curve (see Figure 4). The secant rotational stiffness
300 decrease of 38 % and 75 % respectively with plywood and PVC. This reduction is more
301 significant than for non-stiffened extended end-plates, however similar conclusions could be
302 drawn for thermal breaks attached to a steel support [13]. In fact, the centre of compression
303 positioned close to the bottom end-plate in absence of intermediate layer, for PB-2, gets closer
304 to the beam centre in presence of PVC and plywood. The lever arm decrease and consequently
305 the rotational stiffness. This phenomena is less pronounced for non-stiffened extended end-
306 plates. The rotation capacity is doubled by the addition of PVC due to its crushing in
307 compression. For the three specimens, the end-plate yields in bending in the tensile area and it is
308 the only source of ductility for PB-2. This intermediate layer yielding in compression is also at
309 the origin of the decrease of the plastic bending moment of 31,5 % and 21 % for plywood and
310 PVC, respectively. The addition of PVC also increases the ultimate resistance of 6,4 % mainly
311 because of a decrease of prying effect and of the use of different bolts, partially/fully threaded.

312 The failure of connections PB-2 and RTPB-2-P is caused by bolt rupture in tension whereas that
313 of RTPB-2-B is due to slab reinforcement rupture.

a) PB-2 b) RTPB-2-P c) RTPB-2-B

Figure 7 *– Deformed shape of specimens PB-2, RTPB-2-P/B at failure*

314 The deformed shapes of specimens PB-3 and RTPB-3-P at failure, which corresponds to bolt
315 rupture, are presented in Figure 8. For the two connections, the end-plate remained elastic, the
316 ductility of connections PB-3 is monitored by the bolt elongation characterized by an important
317 reduction of the bending moment after initiation of necking (see Figure 4-c). The rotation
318 capacity of connection RTPB-3-P is increased by PVC crushing in the compressive area. The
319 insertion of the PVC plate reduce the secant rotational stiffness, the plastic and ultimate bending
320 moments of 18 %, 20,3 and 10,1 % respectively. Contrary to the two previous configurations,
321 the addition of intermediate layer decreases the ultimate bending resistance. It can be explained
322 by the fact that prying effects does not develop for the two configurations and different threaded
323 length of the specimen with PVC. Connections PB-4 and RTPB-4-P, which use post-installed
324 chemical fasteners, are depicted in Figure 9 at failure that corresponds to concrete edge rupture.
325 Prying effects does not develop for the two configurations due to the high flexibility of
326 fasteners.

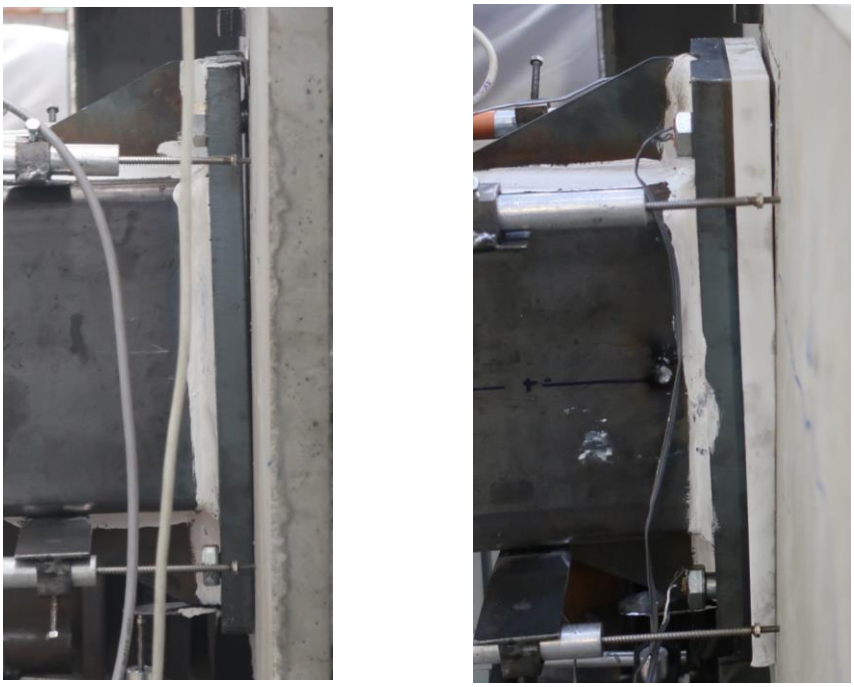

a) PB-3 b) RTPB-3-P

***Figure 8** – Deformed shape of specimens PB-3 and RTPB-3-P at failure*

The secant rotational stiffness is not impacted by the addition of PVC (see Table 4 and Figure 4). Nevertheless the plastic and ultimate bending moments decrease of 30,2 and 17,7 %, respectively. These reductions are caused by the reduction of the lever arm and an early yielding of PVC in the compressive area. The rotation capacity is almost doubled due to PVC crushing in compression but is very limited comparatively to connections fastened to the lintel by bolted embedded end-plates (see Figure 4-f). The geometry of connections of PB-4 and PB-2 are identical except fastening to the concrete block that corresponds to post-installed mechanical fastener and bolted embedded plates, respectively. The ultimate resistance of PB-4 is almost divided by 2 comparatively to PB-2 because of the limited anchoring of the first one. The stiffness is also divided by 3. These differences are typically observed between these two fastening systems. However, in presence of intermediate layers, the difference of plastic bending moment is not significant. Connections using post-installed fasteners are not really affected by the addition of insulating layers because the tensile area is already flexible.

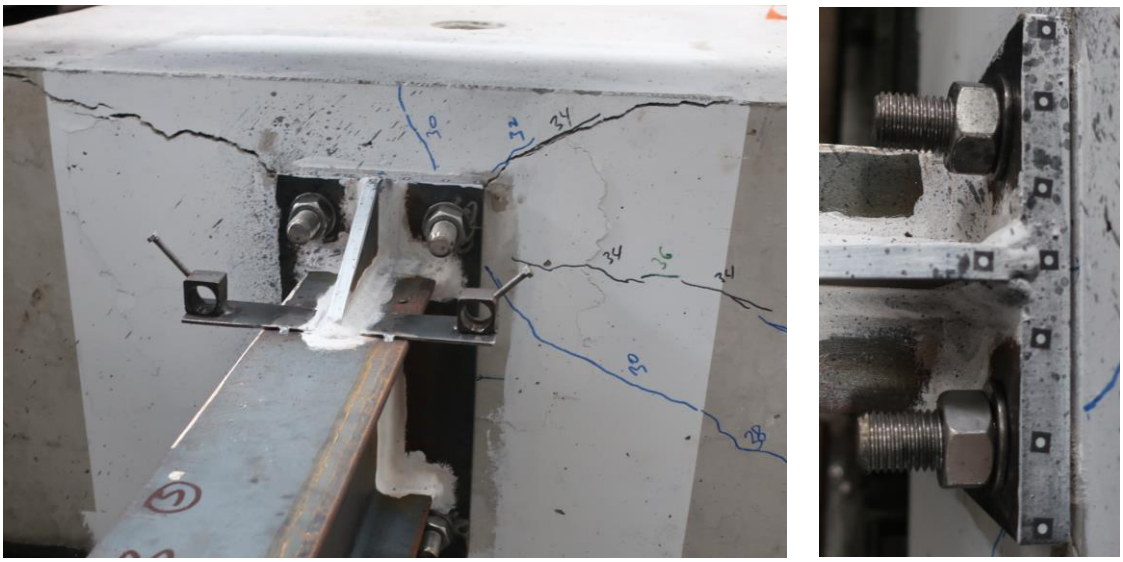

a) PB-4

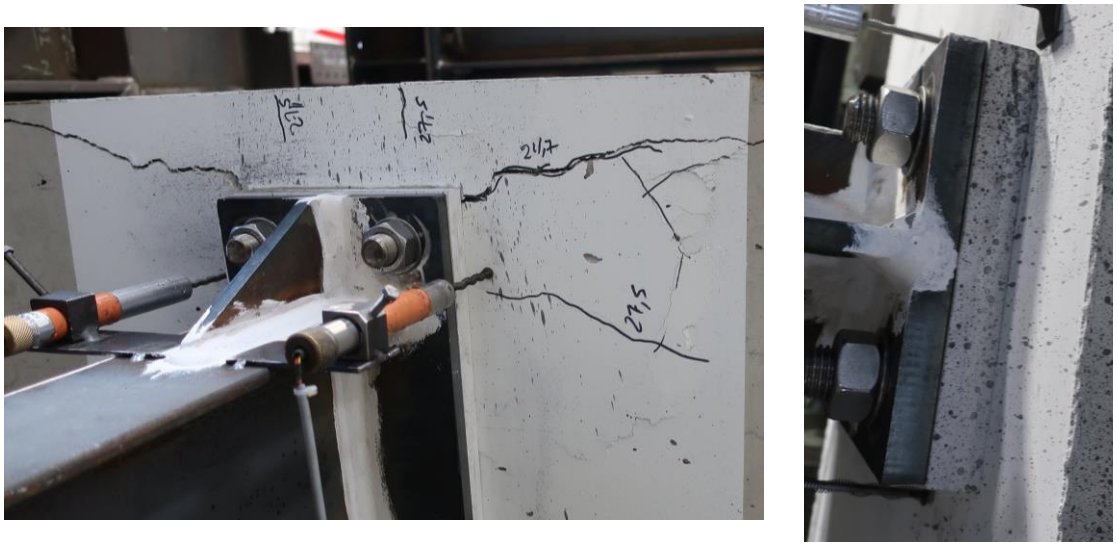

b) RTPB-4-P

Figure 9 *– Specimens PB-4 and RTPB-4-P at failure*

340 The failure mode of connections PB-5 and RTPB-5-P1 starts by anchor sliding in the tensile
341 area and is followed by the concrete cone failure (see Figure 10). Prying effects did not develop
342 for the two specimens due to the flexibility of the mechanical fastener. Nevertheless, the failure
343 pattern is quite different, hence a yield line parallel to the tube develops in the compression area
344 to accommodate the rotation of the connection for PB-5. For the connection with intermediate
345 layer, this rotation is ensured by the PVC crushing in compression, the end-plate deformation is
346 reduced. The concrete lintel started to crack for a bending moment around 4-4,5 kNm. The
347 addition of the PVC layer does not impact the secant rotational stiffness as well as the plastic

bending moment, the flexibility of the connection is mainly affected by the mechanical fastener elongation. The ultimate bending moment decrease of 10%, this reduction can be caused by the modification of the position of the centre of compression.

a) PB-5 b) RTPB-5-P1

Figure 10 *– Specimens PB-5 and RTPB-5-P1 at failure*

2.5. Summary on mechanical tests

The main conclusions that can be drawn from the monotonic mechanical tests are the following:

- The secant rotational stiffness is not strongly affected by the addition of insulating layer in presence of post-installed mechanical/chemical fasteners mainly because the tensile area is already quite flexible. In presence of embedded end-plates, the addition of PVC or plywood can significantly decrease the secant rotational stiffness because these connections are quite rigid without intermediate layer. However the rotational stiffness value was greater than 5000 kNm/rad for connections of beam of 200 mm depth and was largely acceptable for a balcony.

- Except for PB-5, the plastic bending resistance is reduced (between 20 and 40 %) by the addition of intermediate layer whatever the material used. This decrease is due to

yielding of PVC/Plywood in the compressive area. The plastic bending moment of PB-5 is not affected by the addition of PVC probably because the anchoring sliding causes firstly the non-linearity.

- The failure was not affected by the addition of intermediate layer and corresponds to bolt rupture in tension for bolted embedded plates (with reinforced slab) or concrete cone/edge failure for post-installed mechanical/chemical fasteners. The reduction of the ultimate bending moment of the connection was quite limited by the addition of intermediate layer, lower than 20 %. On the contrary, the resistance could be increased by the addition of PVC or plywood mainly because of a reduction of the threaded length and the modification of prying effect.
- The rotation capacity is significantly increased by the addition of intermediate layer whatever the design of connection because of yielding of the layer in the compressive area. The rotation capacity of non-stiffened extended end-plate (connections PB-1 and RTPB-1-P/B) is increased compared to that of stiffened extended end-plate (connections PB-2 and RTPB-2-P/B) as a result of the development of an important plastic yield line parallel to the beam flange. The rotation capacity of connections PB-4 and RTPB-4-P is very limited comparatively to that of PB-2 and RTPB-2-P mainly due to the absence of steel component yielding. The curves of PB-5 and RTPB-5-P1 are quite close mainly because the deformability come mostly from sliding of fasteners in the tensile area.

The behaviour of bolted end-plate connections attached to concrete support with intermediate layer is similar to that obtained with a steel support by Couchaux et al [13] and corresponds to a reduction of the rotation stiffness as well as the plastic bending but to identical failure modes and limited reduction of the ultimate bending resistance. For post-installed fasteners, the effect of the intermediate layer is more limited particularly concerning the rotational stiffness.

3. Fire tests

3.1. Introduction

The fire resistance is generally required for the attached steel structure in façade [14]. In this case, it should ensure the good performance of the attached structure with thermal breaks. The use of specific materials for thermal breaks could lead to a loss of mechanical strength at high temperatures when these items are subjected to the flames coming out of the facade openings. Moreover, the added structure may have a significant role to reduce the risk of fire spread to upper levels. Therefore, it is essential that the sealing hot gases and flames is ensured at the junction of the attached structure and facade. For this reason, two fire tests have been performed on balconies attached with and without thermal breaks that were exposed to external flames generated by a generalized fire in a furnace. The fire test set-up as well as measurements are presented in section 3.2. The tests results are discussed in section 3.3 in term of temperature evolution and beam displacement.

3.2. Fire test presentation

3.2.1. Fire test furnace

Among European countries, several tests exist to assess the impact of flames on a facade. They are oriented toward fire reaction and the LEPIR II, a French large scale test [18], is one of them. It can be used as a basis to test the fire resistance of a structure. The test facility consists in a block usually used for LEPIR II normative tests (experimental test facility with two levels under natural fire). For a LEPIR II test, the furnace has two blocks : one for the ground level, the other for the upper level. Each block has two standardized openings. In the present tests, only the ground block is used and slight modifications have been done.

The internal dimensions of the furnace are 2850×4850×2500 mm. The front face is closed with a 200 mm thick concrete block, and at the top, the reinforced concrete slab is 250 mm

416 thickness, with a lintel of 600 mm high. The front face had one opening of dimensions
417 2000×1500 mm, located at 950 mm from the ground (see Figure 12-a).

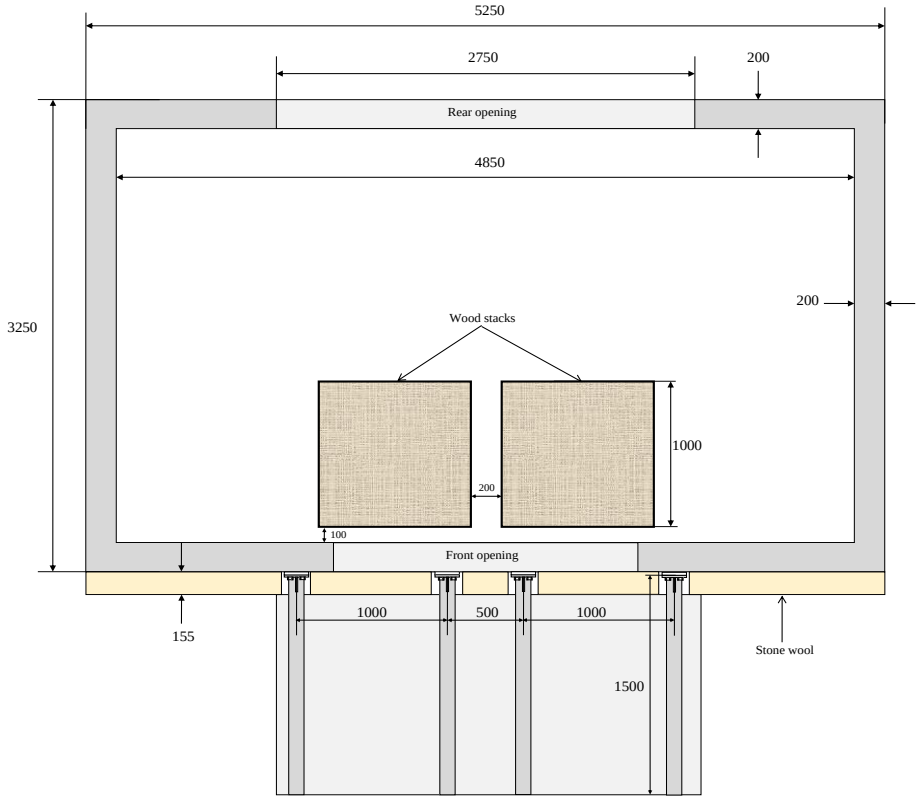

a) Plan view

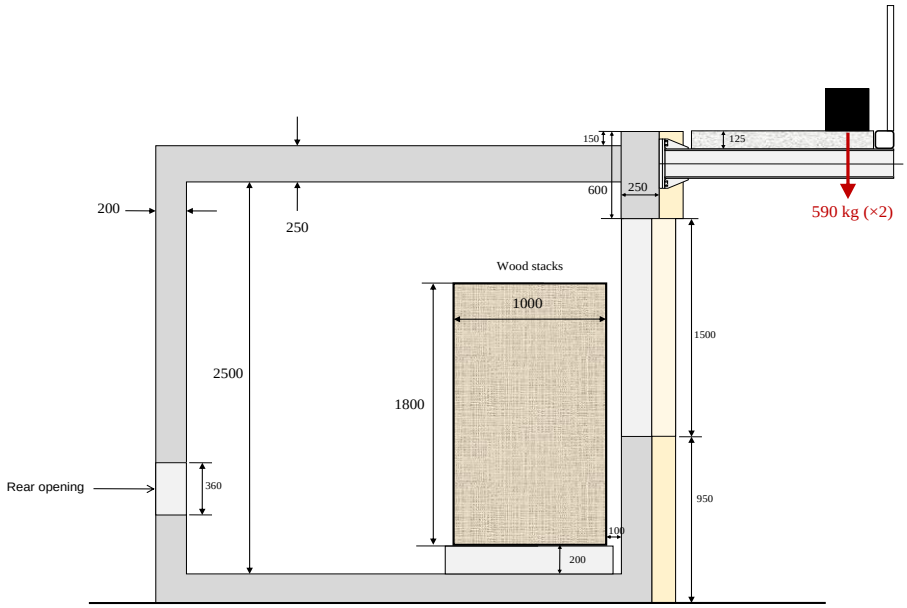

b) Lateral view

Figure 11. *Plan and lateral view of the test set-up (dimensions in mm)*

418 This size allows to have two balconies per test and also to have one of the beams highly
419 exposed to fire. A LEPIR II tests involves two openings of 1000×1500 mm. Thus, the opening
420 area is the same and also the ventilation. The rear face had an opening of dimensions 2750×360
421 mm (see Figure 12-b) in its lower part used for air supply. It allows also the ignition of the
422 wood stacks.

a) Front opening b) Rear opening

Figure 12. *Test furnace before implementation of balconies*

423 The fire load in the furnace consists of two wood stacks of 300 kg composed in the same way as
424 for a LEPIR II test. This is also consistent with recommendations in the European Standard EN
425 1991-1-2 [19] and the French national annex [20]. Cribs are made of softwood with density 480
426 ± 50 kg/m^3 and moisture content between 9% and 15%. Each crib consists in 3 stacked piles.
427 For each crib, the total dimensions are 1000×1000×1800 mm. The cribs are located at 100 mm
428 from the front wall, 200 mm above the ground and at a distance of 200 mm from each other (see
429 Figure 13).

Figure 13. *Wood stacks*

3.2.2. Fire test configuration

Due to the dimensions of the test cell, two balconies were connected and characterized for each test:

- Balconies B1-1 and B1-2 during test n°1,
- Balconies B2-1 and B2-2 during test n°2.

The balconies tested had a range of 1,5 m and were supported by two consoles separated by a distance of 1 m. The beams are composed of IPE 200 of steel grade S275 and of end-plate in S235. The geometry is similar to connections PB-4 and RTPB-4-P tested under monotonic loading (see Figure 2-d) that develop the lower mechanical properties under monotonic loading for the connection of beams of 200 mm height.

The beams positioned in front of the opening were significantly exposed to flames while the other one's had a more limited exposition. The consoles were installed on a reinforced concrete lintel of 600 mm high. The connections were fastened to the lintel with four chemical post-installed fasteners M20 HIT-Z-R. The balcony slab was in cellular concrete with a thickness of 125 mm and a density of 550 kg/m^3. The external thermal insulation of the facade is made of 140 mm stone wool with a finishing coat of 15 mm.

447 ***Table 5.*** *Fire test configurations*

Test	Balcony	Connection	Beam	Insulating	t_a (mm)	Additional external insulation
Test n°1	B1-1	PB-4	IPE200	No	-	No
	B1-2	RTPB-4-P	IPE200	PVC	20	No
Test n°2	B2-1	RTPB-4-B	IPE200	Plywood	30	No
	B2-2	RTPB-4-P	IPE200	PVC	20	Yes

448

449 The balcony without thermal break, balcony B1-1, constitutes the reference case and is
450 representative of a balcony commonly used in practice. Then two configurations have been
451 tested without the addition of external insulation around the connection (right beam in Figure
452 14-b).

a) Global view

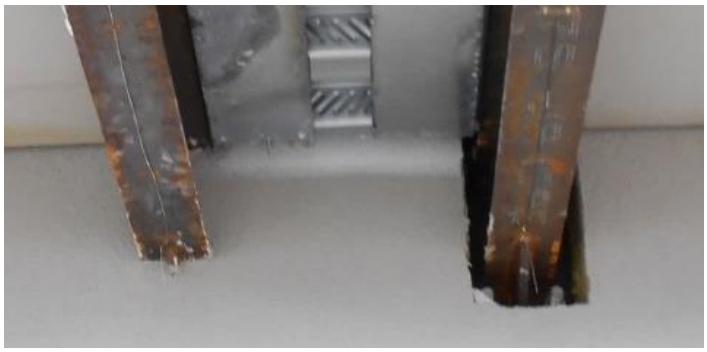

b) Local view

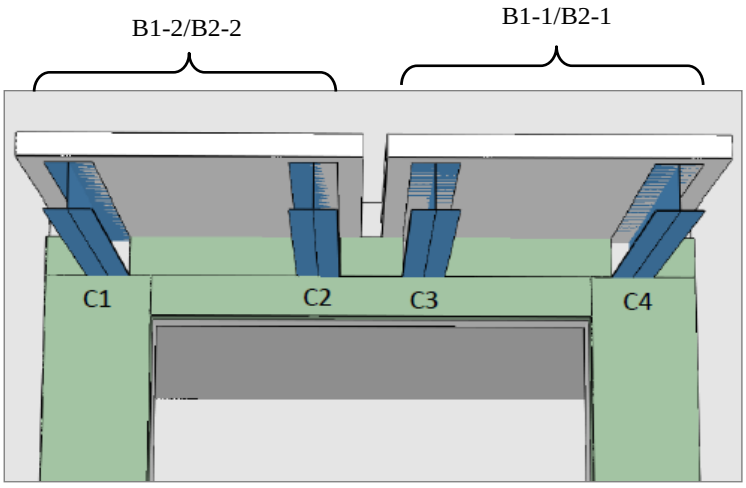

c) Beam labelling

Figure 14. *Balconies and test cell before fire test*

These configurations labelled balcony B1-2 and B2-1 used PVC and plywood, respectively. In practice, this additional insulation is used, the objective of this test was to highlight the impact of this implementation on the performance of the proposed solutions of thermal break. For this reason a last configuration, balcony B2-2, was tested with PVC and additional external insulation around the connection (left beam in Figure 14-b). PVC was chosen because it is more prone to mechanical degradation at high temperature than plywood. The thickness of PVC and plywood layers was equal to 20 and 30 mm, respectively.

The load applied on each balcony was close to 590 kg and distributed on the upper face of the cellular concrete slab at the end of the consoles (see Figure 15). This position is conservative as the connection bending moment is overestimated comparatively to a uniformly distributed load. This load have been designed considering the fire combination $G+\Psi_1 Q$, with $\Psi_1 = 0{,}5$. The total mass per unit area of a balcony, equal to 475 kg/m^2, is thus equivalent to a permanent load (G) of 300 kg/m² and live loads of 350 kg/m² (Q) according to EN 1991-1-1 [17], in the fire combination $G+\Psi_1 Q$. This loading is typical of balconies with a common concrete slab.

Figure 15. *Load applied on the slab of balconies*

3.2.3. Measurements

A total of 25 to 30 thermocouples was positioned on each beam to measure evolution of the temperature during the fire test (see Figure 16). Thermocouples W, X and Y measure the air temperature below the beam. Moreover, temperatures in the test cell were measured and 6 thermocouples were placed under the front opening to measure external flames temperature.

The temperature of beam web/flange is measured by thermocouples I to T. In addition, the objective being to study the behavior of the thermal break, thermocouples (from A to H) have been positioned to measure the temperature at the lintel/layer interface, and layer/end-plate interface. By the end, thermocouples U and V were placed to measure the external insulation temperature. In the following, beams were labelled C1 to C4 (see Figure 14-c). Beams C3 and C4 corresponds to balconies B1-1/B2-1, C1 and C2 to balconies B1-2/B2-2. In addition, a gauge heat flux was positioned at 3 m in front of the opening, and a video camera recorded the tests.

The mechanical behavior of balconies during the fire tests was also a key aspect and particularly the response of the connections. Vertical displacement at the top of the beams, V_{edge}, was measured, as well as the rotation of the connection with an inclinometer, I_c.

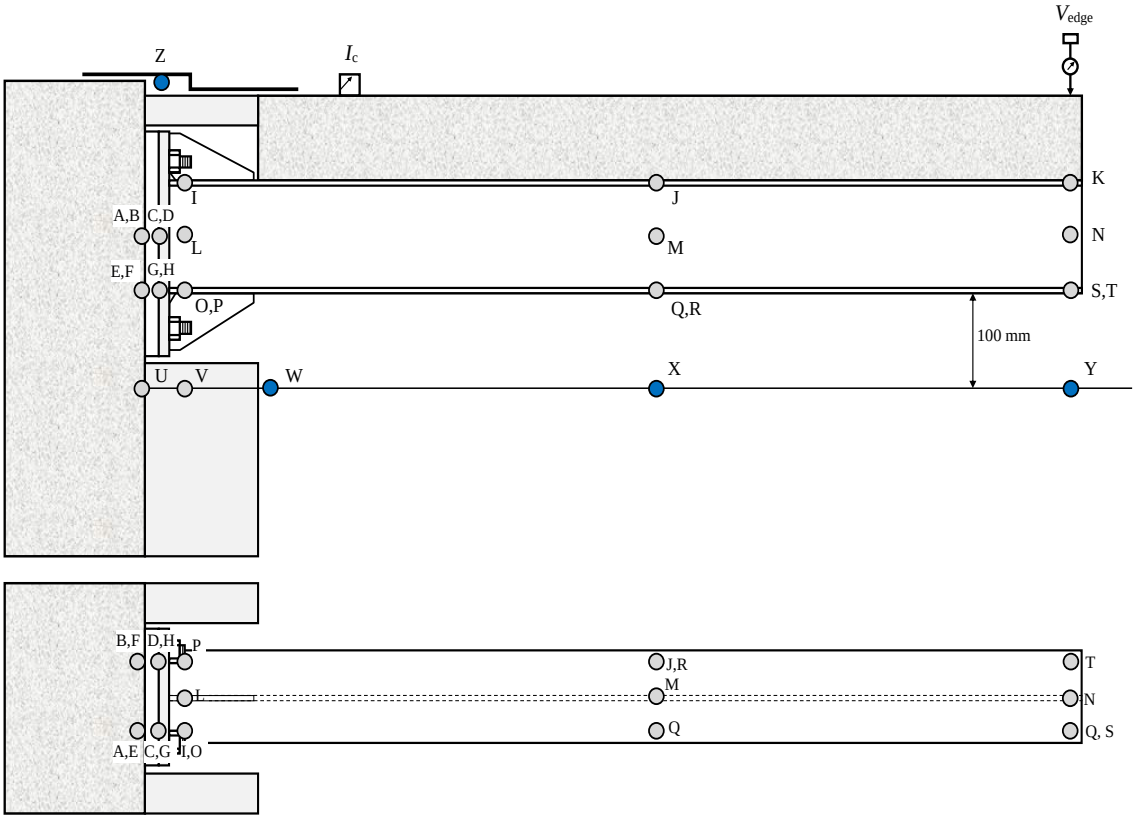

***Figure 16**. Thermocouples and displacement positions*

3.3. Fire test results

3.3.1. Test description

Each test lasts approximately 45 minutes and proceeds as follows (see Figure 17):

- Fuel tanks placed under the wood stacks ignited the fire.
- Smoke exits through the opening of the facade one minute after ignition (see Figure 17-a).
- After 5 minutes, the first external flames appeared (see Figure 17-b).
- At 10 minutes, the fire fully developed and the flames reached their maximum length left the opening with an angle of 45° (see Figure 17-c). Thus, these flames directly impact half of the console.
- From 15 minutes, the fire gradually decreases, and the stacks begin to collapse (see Figure 17-d).
- At 25 minutes, the wood stacks collapsed and no flame was visible outside (see Figure 17-e). Hot gases continue to escape through the opening of the facade, and the temperature under the balcony remains high for another 20 minutes.

a) 1st min

b) 5th min

c) 10th min

d) 15th min

e) 25th min

f) End of test

***Figure 17**. Flame development during test n°2*

Measurement acquisition was cut off after 45-50 minutes. There was no longer any visible flame above the collapsed wood stacks. For the two tests, the stability of balconies was ensured. However, the vertical displacement of balcony B1-2 equal to 144 mm was substantial comparatively to other configurations.

The weather conditions are quite different during the two tests (see Table 6) and this explains the difference concerning the maximal temperature of gases measured (see section 3.3.2).

***Table 6.** Weather parameters*

Test	Temperature	Air Humidity	Wind
	°C	%	km/h
Test n°1	22	45	15
Test n°2	9	73	23

3.3.2. Global temperature evolution

The temperature in the test cell reached 900° when the fire fully developed. The temperature of flames and gases through the front opening was close to 800-900°C under the consoles directly above the opening (Thermocouples, or Tc, W, X, Y) C2 and C3. Temperatures were logically higher under those beams (C2 and C3) than under the C1 and C4 external beams, which were less exposed (see Figure 18). These temperatures are quite close to that obtained with ISO 834 until 25 min particularly during the first test.

In the first part of tests, gas temperature close to the facade (Tc W) is lower than at mid-range and at the extremity (Tc X and Y). This phenomenon is due to the flame tilting through the opening (see Figure 19). At 18 minures, a sharply increase of the temperature is measured up to 25 minutes for the two tests and particularly test n°1. This phenomenon may be due to the collapse of the wood stacks which causes momentarily a greater heat release, and therefore higher temperatures under the consoles C2 and C3. The temperature in the external insulation of the facade above the opening increases progressively during the test. It reaches 600 °C in the heart of the external insulation (thermocouple Tc V), but only 100 °C at the interface between the insulation and the concrete support (Tc U). These measures highlight the importance of external insulation and its proper implementation around beams, even in case of exceptional fire situation.

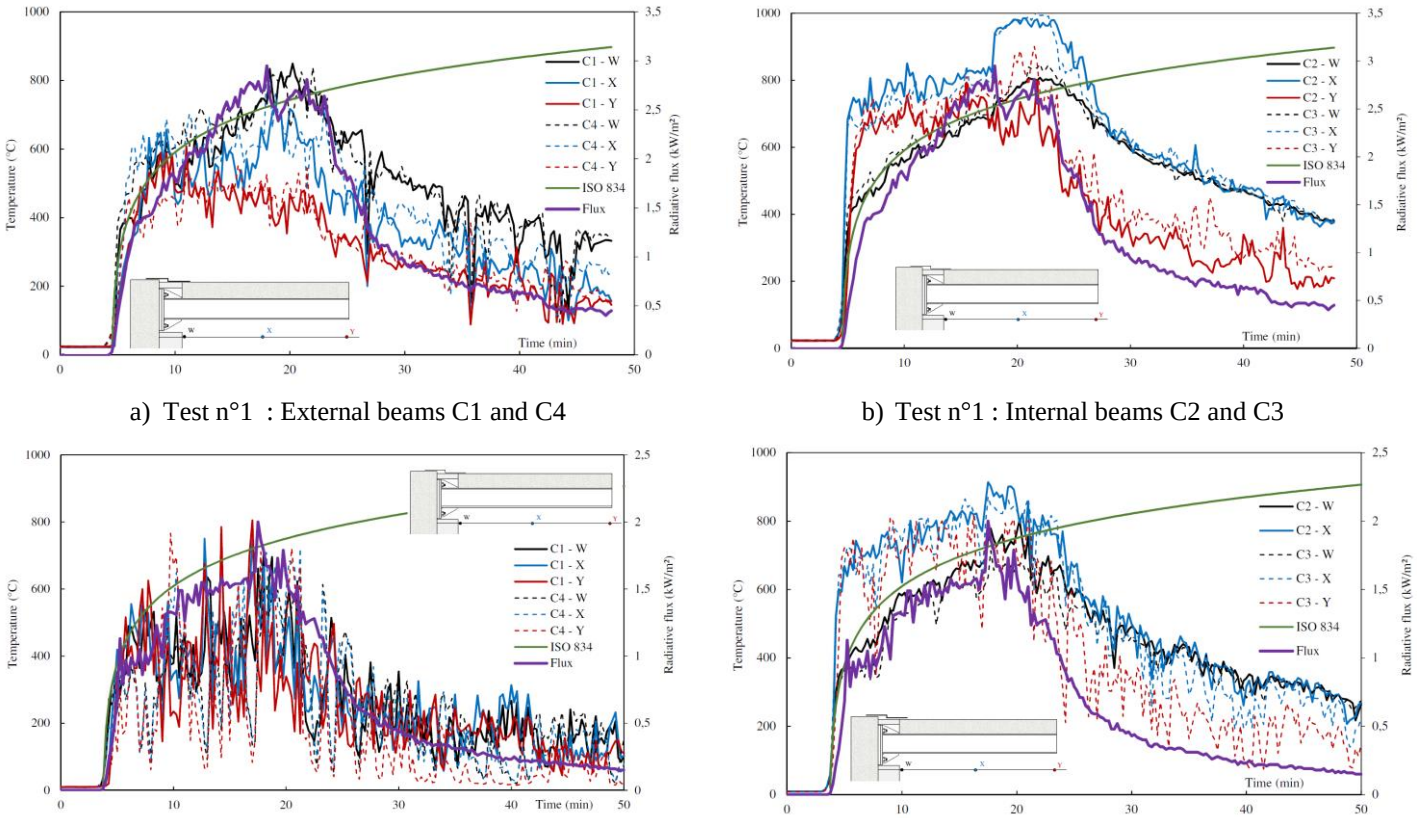

a) Test n°1 : External beams C1 and C4

b) Test n°1 : Internal beams C2 and C3

c) Test n°2 : External beams C1 and C4

d) Test n°2 : Internal beams C2 and C3

Figure 18*. Gas temperature of flames through the opening (Tc W, X, Y)*

Figure 19. *Flames through the opening (test n°1 – 17 min)*

The central beams located directly above the opening were the most exposed. In the same way as for gas temperatures, the temperature of steel section closest to the facade was lower than the temperature at mid-range or at the beam extremity, namely 400-500°C (Tc O) versus

700-900°C (Tc Q, S). The highest temperature is at mid-range (Tc Q). At mid-range and at the extremity, the steel temperatures follow the gas temperature (see Figure 20). The maximum temperature of the end-plate connections (Tc O) was around 500 °C when they were exposed to flames and only 200°C for the end-plate connections protected by the additional external insulation (Test n°2, beam C2 in Figure 20-b).

The temperatures were homogenous through the steel beam section. Web and lower flange temperatures were very close, the temperature of the upper flange is slightly lower (approximately 100°C) because the concrete slab slows the heating.

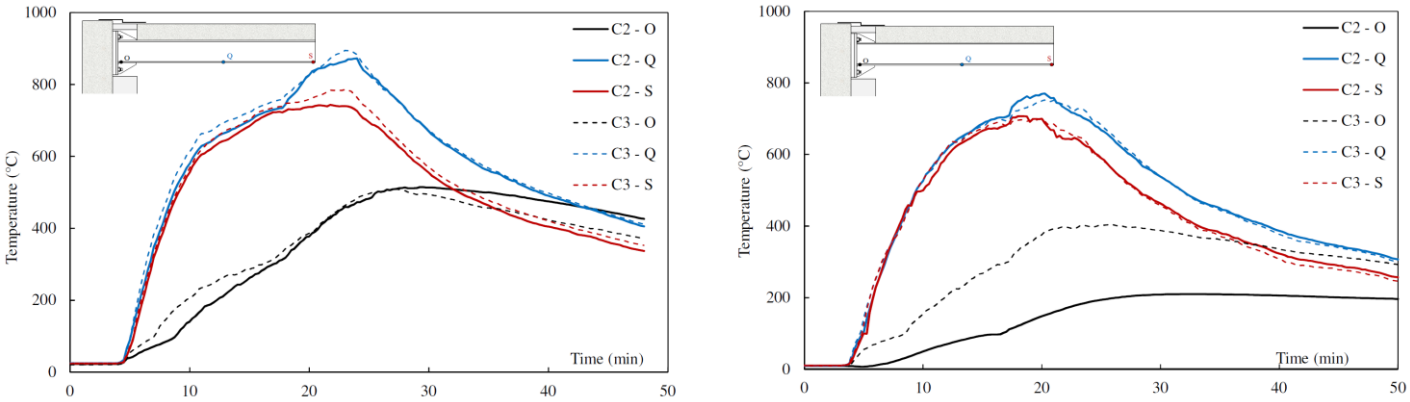

a) Test n°1 : Internal beams C2 and C3 b) Test n°2 : Internal beams C2 and C3

***Figure 20**. Lower flange temperature at facade (Tc O), mid-range (Tc Q) and extremity (Tc S)*

3.3.3. Connection fire behaviour

The evolution of the temperatures measured at the interface between the lintel and the intermediate layer (Tc E and F), and between the layer and the end-plate (Tc G and H) is depicted in Figure 21. For connections without intermediate layer, the temperature of the interface between the end-plate and the lintel is only provided (Tc E and F). The maximal temperature measured at interfaces as well as the maximal displacement are also added in Table 7. The maximal air temperature measured by Thermocouple W is also added.

551 ***Table 7.*** *Maximal temperatures and displacements*

Test	Balcony	Intermediate layer	Additional external insulation	Air temperature (°C)	Layer/endplate temperature (°C)	Lintel/layer temperature (°C)	V_{max} (mm)
Test n°1	B1-1	No	No	848	375		58
	B1-2	PVC - 20 mm	No	807	449	281	144,6
Test n°2	B2-1	Plywood – 30 mm	No	713	320	51	43,4
	B2-2	PVC – 20 mm	Yes	804	164	32	58,1

552

553 By comparing balconies B1-2 and B2-2, the influence of the additional external insulation is
554 clearly highlighted: the decrease between the air temperature (Tc W) and the end-
555 plate/intermediate layer interface temperature (Tc G, H) goes from 358°C (807°C-449°C)
556 without the additional external insulation, to 640°C (804°C-164°C) with additional external
557 insulation. For balcony B2-2, with external thermal insulation, the temperature at the interface
558 between the end-plate and the layer is lower than that between the layer and the lintel for
559 balcony B1-2 that do not use external insulation.

560 The presence of intermediate layer plays also a role in the temperature decrease at the lintel
561 interface (Tc E, F). In the reference case (without thermal break), the maximal end-plate/lintel
562 temperature interface is equal to 375°C. The plywood intermediate layer allows a decrease of
563 this temperature to 50°C even without additional external insulation around the connection.
564 With PVC intermediate layer and additional external insulation around the connection, this
565 temperature decreases to 30°C. The interface temperatures continues to increase very slowly
566 after the end of the fire pick because of thermal conductivity (see Figure 21-d).

567 However for balcony B2-1, with PVC and no external insulation, this decrease is more
568 limited, the maximal temperature of the layer/lintel interface was around 280 °C mainly because
569 the PVC intermediate layer was partially melted and consumed (see Figure 22-a and Figure 23-
570 a/b). With the deteriorating of the intermediate layer, hot gases were introduced and heated the
571 lintel (see Figure 22-a). This partial consumption, non uniform, induces the rotation of the end-
572 plate and as a consequence a significant vertical displacement equal to 144 mm at the top of the

beam, against 44-58 mm for the other configurations. However, this deformation that causes a rotation of the end-plate did not affect the overall stability of the attached beam.

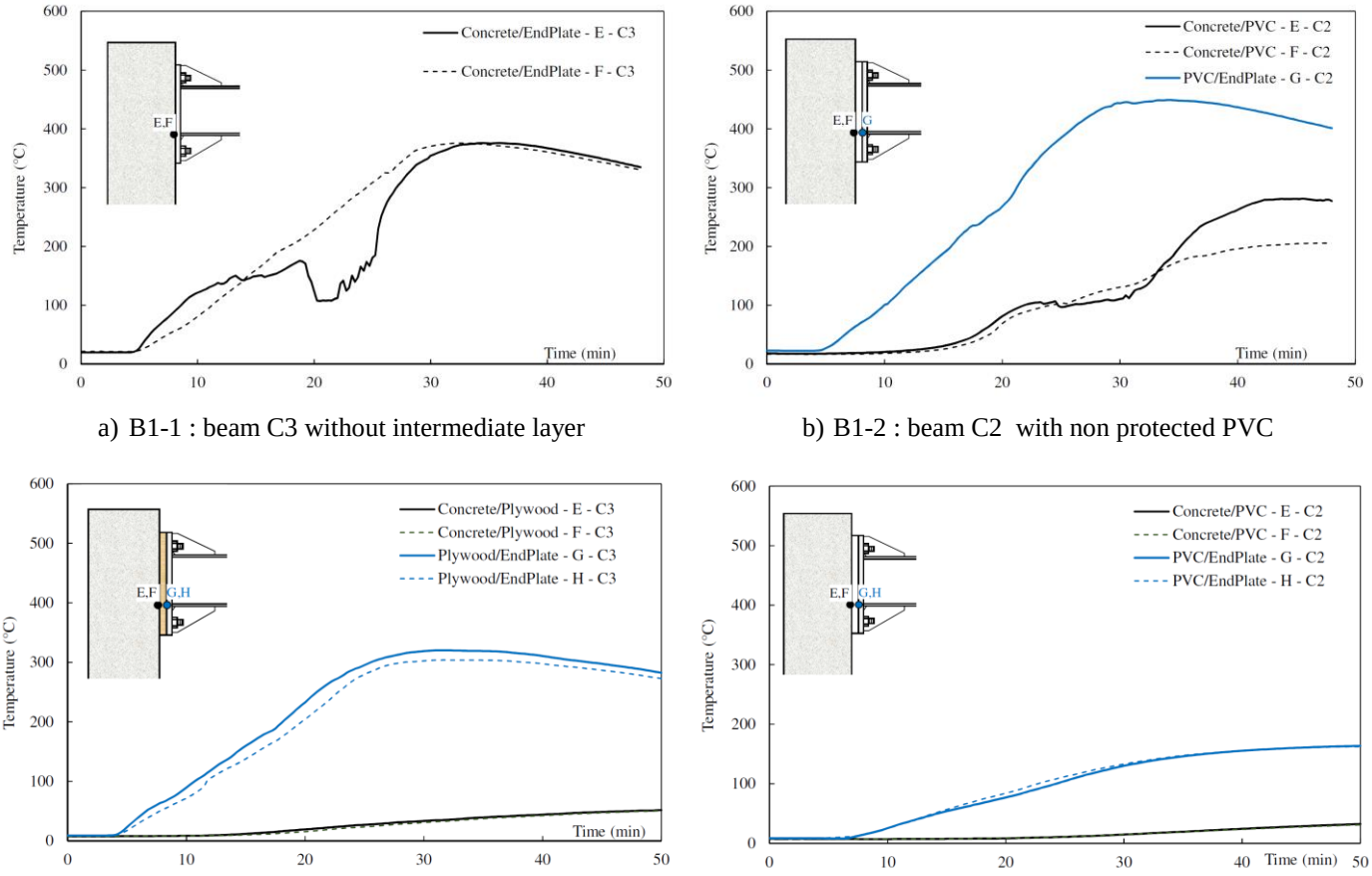

a) B1-1 : beam C3 without intermediate layer

b) B1-2 : beam C2 with non protected PVC

c) B2-1 : Beam C3 with non protected plywood

d) B2-2 : Beam C2 with protected PVC

Figure 21. *Temperatures of layer/end-plate (Tc G, H) and layer/lintel (Tc E, F) interfaces*

The plywood layer started to burn (see Figure 23-c) but only at the interface between the end-plate and the layer (see Figure 22-b). This layer keep its thickness and the maximal displacement at the top of the balcony does not exceed 43,4 mm. This balcony was the less impacted by the fire despite the absence of additional external insulation around the connection.

a) PVC, no External Insulation b) Plywood, no external insulation c) PVC and external insulation

Figure 22. *Connections after fire test*

For balcony B2-2 with PVC and additional external insulation, the PVC did not burn (see Figure 23-d) but its thickness decrease in the compressive area (see Figure 22-c) due to a reduction of its mechanical properties at high temperatures (around 160 °C). The nut of bottom anchor bolts is no more in contact with the end-plate. This reduction of the PVC thickness in the compressive area also induce a global rotation of the connection and maximal displacement of the edge of the balcony of 58 mm. A similar displacement has been obtained for balcony B1-1 without thermal break and additional external insulation around the connection. A thermal break using PVC and additional external insulation is able to develop a fire behaviour close to that of a conventional connection (without intermediate layer and additional external insulation). The solution with plywood layer but without additional external insulation permit to draw the same conclusions.

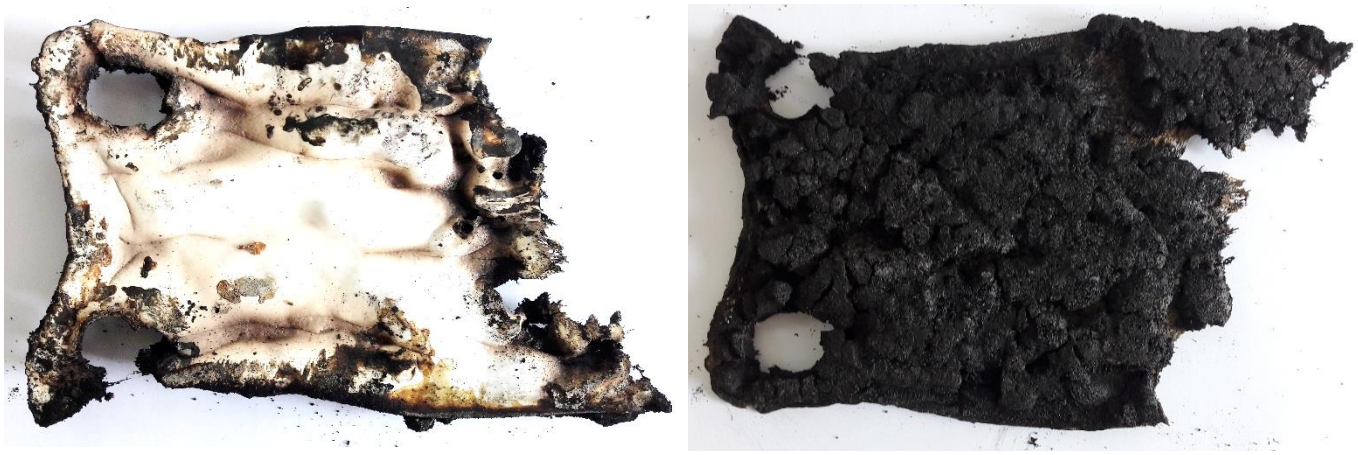

a) Test B1-2 : PVC surface in contact with the lintel

b) Test B1-2 : PVC surface in contact with the end-plate

c) Test B2-1 : Plywood surface in contact with the end-plate

d) Test B2-2 : PVC layer

Figure 23. *Intermediate layer after fire test*

590 The evolution of the displacement measured at the top of the balcony is presented in Figure
591 24-a. In addition, this displacement is given in Figure 24-b in function of the temperature
592 measured at the interface between the end-plate and the layer or concrete for B1-1. Except for
593 balcony B1-2, with PVC and no external insulation, the maximal displacement is around 40-60
594 mm. For balconies without thermal break, B1-1, and PVC but without additional external
595 insulation, B1-2, the increase of the displacement is quite fast and tends to an asymptote after
596 20-25 min. For the two other balconies, the increase of the displacement is slower as well as the
597 temperature at the interface between the layer and the end-plate (see Figure 21). We can clearly
598 observe with Figure 24-b that for the two first specimens, the displacement is stabilized for a
599 temperature of 200-300 °C. When the temperature decrease, the displacement is not modified.
600 On the contrary for plywood, temperatures greater than 300° do not affect strongly the
601 displacement. The displacement continues to increase even after the temperature decrease
602 because of the plywood burning. For balconies with PVC and additional external insulation, the
603 temperature is lower than 200 °C and the combustion didn't start as well as major rotation of the
604 connection. Nevertheless, the displacement-temperature curves obtained in presence of PVC
605 layer with and without additional external insulation are almost parallel (see Figure 24-b).

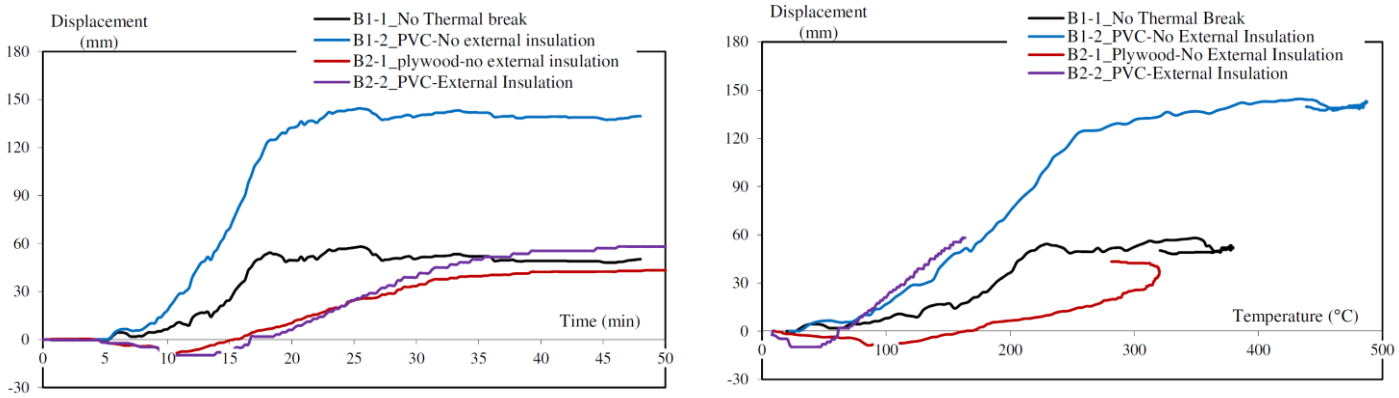

a) Evolution during fire test b) Effect of temperature at interface with end-plate

Figure 24*. Vertical displacement of the edge of the balcony*

606 ### *3.4. Summary on fire behaviour*

607 The in situ fire tests highlighted the impact of the different connections configurations,
608 previously tested at ambiant temperature, on the global behaviour of the balcony. The balcony

directly attached to the concrete support without additional external insulation behaves very well under this fire senario and the maximal displacement was limited to 58 mm. The addition of intermediate layer composed of PVC or plywood didn't affect this stability even in absence of external thermal insulation around the connection. Without additional external insulation, the PVC layer burns partially loses its thickness that generates a global rotation of the connection and an important displacement at the top of the balcony of 144 mm. The plywood starts to burn but keeps its integrity, the rotation was clearly more limited and as a consequence the top displacement was equal to 44 mm. This latter was lower than that obtained with the conventional connection in absence of thermal break but also of additional external insulation. The addition of external insulation around the connection permits to avoid PVC burning and limit significantly the global rotation of the connection. The use of intermediate layer such as plywood isolates strongly the lintel and reduces the temperature, this phenomena can be amplified by the addition of external insulation around the connection.

4. Conclusions

This paper gives the results of a study assessing the mechanical and fire behaviour of simple solutions of thermal breaks for external steel structures (balconies, solar panels …) attached on a concrete facade with External Thermal Insulation. The studied solutions are composed of a PVC or plywood layer implemented between attached steel structures and support. The main advantages of these solutions compared to manufactured products proposed by industrial suppliers are their reduced costs and ease of erection.

Experimental tests performed on the proposed solutions loaded monotonically under bending moment highlighted that the mechanical properties of these solutions are close to that of standard connections directly fastened to the concrete support. The decrease of the ultimate bending resistance is hence quite limited. On the contrary, the plastic bending resistance decrease substantially due to the early yielding of the insulating layer in the compressive area. The same phenomena was also observed for thermal breaks attached to a steel structure [13].

The secant rotational stiffness decreases due to the addition of intermediate layer but the values obtained, greater than 5000 kNm/rad for connections of beam of 200 mm depth, were largely sufficient for the connection of a balcony. For post-installed mechanical/chemical fasteners, the addition of insulating layer did not modify the rotational stiffness but decrease slightly the ultimate bending resistance. Connections with bolted embedded end-plates were able to develop large bending resistances compared to post-installed fasteners.

In order to evaluate the influence of the thermal breaks on the behaviour of a balcony under fire, external flame experiments were carried out. These tests have demonstrated that the studied solutions of thermal break does not affect the stability of the balconies under fire. These results remain valid even in absence of external insulation around the connections leading to a direct exposure of the thermal break to flames. Plywood starts to burn but keeps its integrity and initial thickness. On the contrary, the PVC of non protected connections burns, generates a global rotation of the connection and thus a large displacement of the balcony but without collapse. With additional external thermal insulation, temperature of the assemblies remains low and avoids PVC burning. Thus, a correct implementation of the proposed solution (*ie* with additional external thermal insulation around the connection) is strongly required.

The experimental campaigns performed on the proposed solutions of thermal attached to steel [13] and concrete supports highlighted that the mechanical and fire behaviours are close to that of conventional connections directly fastened to the support. Nevertheless, design methods are necessary to ease the application of these solutions in practice. The calculation of the rotational stiffness as well as the plastic/ultimate bending resistances are of primary importance. The contact distribution being different from standard connections in the tensile and compressive area, new analytical models can potentially be developed. By the end, the long-term effect should be considered particularly for the evaluation of the rotational stiffness.

Acknowledgments

This research was partially funded by ADEME (Environment and energy management Agency) with the contract ADEME n°1704C0003. The project consortium was composed of CTICM, INSA Rennes and PERRAUD.

5. References

[1] Directive 2010/31/EU of the European parliament and of the council of 19 may 2010 on the energy performance of buildings.

[2] Ben Larbi A., Statistical modelling of heat transfer for thermal bridges of buildings. Energy and Buildings 37/9, 945 – 951, 2005.

[3] EN ISO 10211, Thermal bridges in building construction. Heat flows and surface temperatures. Detailed calculations, 2017.

[4] Ge H., McClung V.R., Zhang S., Impact of balcony thermal bridges on the overall thermal performance of multi-unit residential buildings: A case study, Energy and Buildings 60, p.163-173, 2013.

[5] Nasdala L., Hohn B., Rühl R., Design of end-plate connections with elastomeric intermediate layer, Journal of Constructional Steel Research, Vol. 63, p. 494-504, 2007.

[6] Sulcova Z., Sokol Z., Wald F., Structural connections with thermal separation, CESB 07 Prague Conference, p.672-677, 2007.

[7] Cleary D.B., Riddell W.T., Camishion N., Downey P., Marko S., Neville G., Oostdyk M., Panaro T., Steel connections with fiber-reinforced resin thermal barrier filler plates under service loading, Journal of Structural Engineering, Vol 142, No11, 2016.

[8] Peterman K. D., Kordas J. A., Moradei J., Coleman K., D'Aloisio J. A., Webster M. D., Hajjar J. F., "Thermal Break Strategies for Cladding Systems in Building Structures: Report to the Charles Pankow Foundation," Boston, MA, 2016.

683 [9] Peterman K.D., Kordas J., Webster M.D., D'Aloisio J.A., Hajjar J.F., Structural
684 performance of axially and laterally loaded cantilevers with thermally-improved
685 detailing, Journal of Constructional Steel Research, Vol 181, 106617, 2021.

686 [10] Hamel S., White S., Thermo-mechanical modelling and testing of thermal breaks in
687 structural steel point transmittances, Anchorage, AK, 2016.

688 [11] Ben Larbi A., Couchaux M., Bouchaïr A., Thermal and mechanical analysis of thermal
689 break with end-plate attached steel structures, Engineering structures, Vol 131, p.362-
690 379, 2017.

691 [12] Report DRV/16-RCM-107/002-B, Treatment of singular points in energy efficient
692 buildings, Project ADEME TREPOS, October 2019 (in French).

693 [13] Couchaux M., Ahlasawi A., Ben Larbi A., Monotonic and cyclic tests on beam to column
694 bolted connections with thermal insulation layer, Engineering Structures, Vol 204,
695 109621, 2020.

696 [14] Morgado H.J.L., Rodrigues J.P.C., Balcony effect on the external fire spread into upper
697 floors, Journal of structural fire engineering, Vol.6, No.4, p.255-273, December 2015.

698 [15] ECCS, Recommended testing procedures for assessing the behavior of structural elements
699 under cyclic loads, European Convention for Constructional Steelwork, Technical
700 Committee 1, TWG 13 – Seismic Design, No45, 1986.

701 [16] Yang F., Veljkovic M., Liu Y., Fracture simulation of partially threaded bolts under
702 tensile loading, Engineering Structures, Vol 226, 111373, 2021.

703 [17] Grimsmo E.L., Aalberg A., Langseth M., Clausen A. H., Failure modes of bolt and nut
704 assemblies under tensile loading, Journal of Constructional Steel Research, Vol 126,
705 p.15-25, 2016.

706 [18] IT 249 - Rules of Fire Safety and Panic in Establishments Open to Public, Journal
707 Official of the Republic of France, France, 2010 (in French).

[19] EN 1991-1-2: Eurocode 1: Actions on structures – Part 1-2: General actions – Actions on structures exposed to fire.

[20] French Natinal Annex to EN 1991-1-2: Eurocode 1: Actions on structures – Part 1-2: General actions – Actions on structures exposed to fire.

[21] EN 1991-1-1: Eurocode 1: Actions on structures – Part1-1: General actions – Densities, self weight, imposed loads for buildings

715

Appendix A

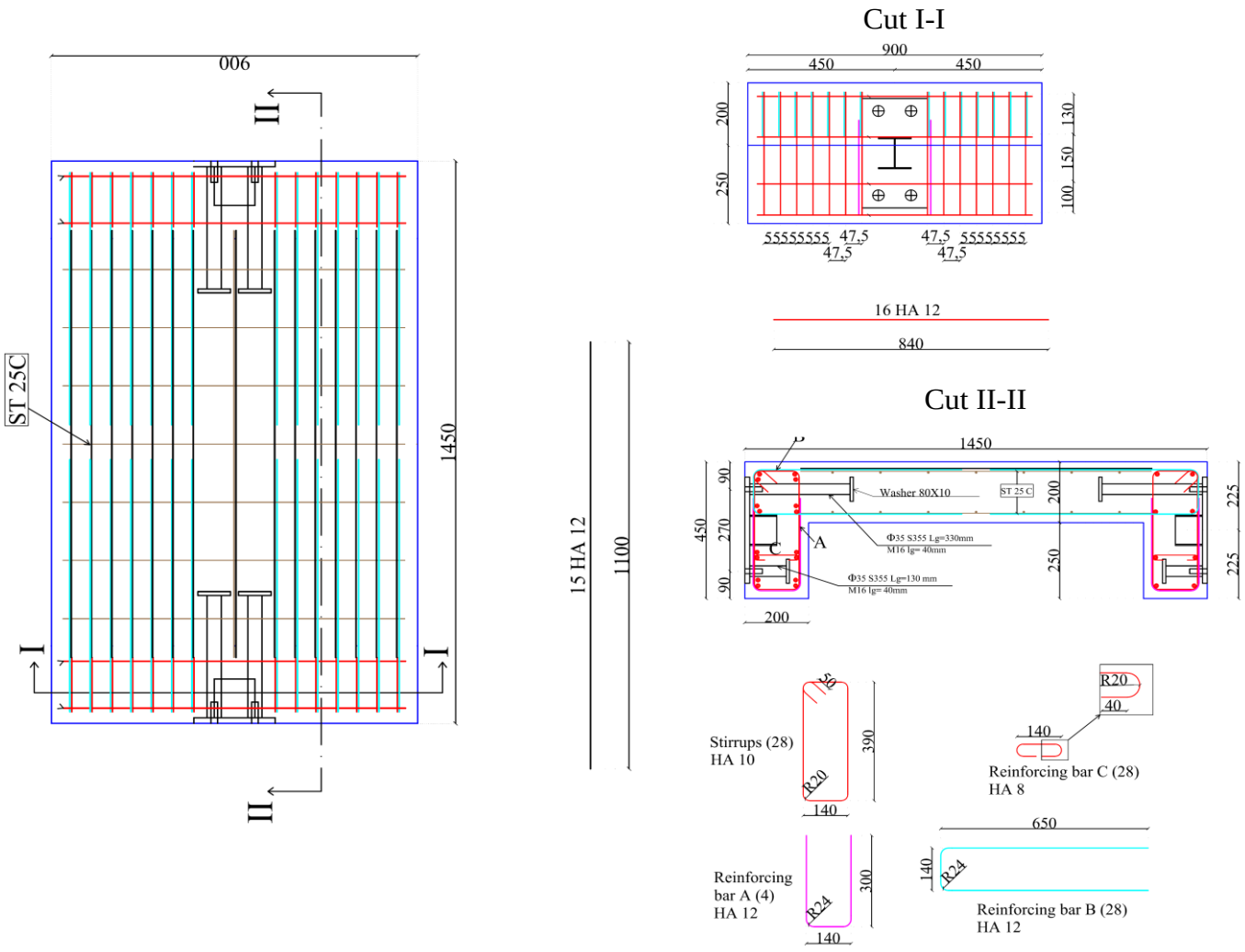

Figure A.1. *Reinforcement of concrete Block B1*

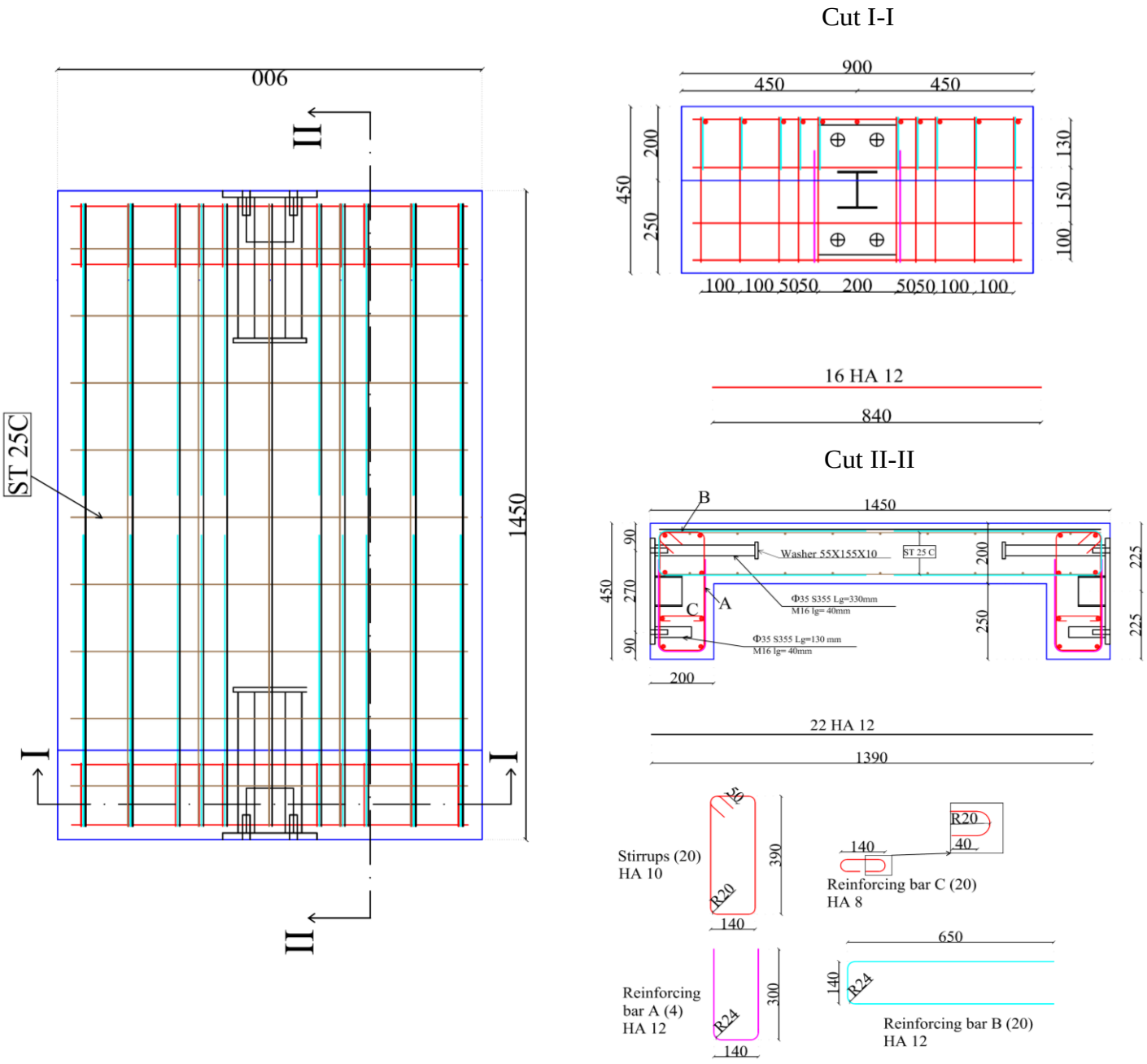

Figure A.2. *Reinforcement of concrete Block B3s*

716